Geosystems and Geoenvironment 5 (2026) 100521

Contents lists available at ScienceDirect

Geosystems and Geoenvironment

journal homepage: www.elsevier.com/locate/geogeo

Delineation of groundwater potential zones in Garowe district, Puntland, Somalia, using remote sensing and GIS-based analytical hierarchy process

Ahmed Mohamed Ismail[a,b,c,*], Farah Jama Farah[b], Mohamed Abdi Jama[c], Rodgers Makwinja[d], Yoshihiko Inagaki[e]

[a] Africa Center of Excellence for Water Management, College of Natural and Computational Science, Addis Ababa University, P.O. Box 1176, Addis Ababa, Ethiopia

[b] Puntland State University, College of Engineering and Technology, Department of Water Resource Management, Garowe, Puntland, Somalia

[c] East Africa University, College of Postgraduate Studies, Department of Water Management, Garowe, Puntland, Somalia

[d] Institute for Sustainability and Corporate Citizenship, University of South Africa, P.O. Box 392, UNISA 0003, Pretoria, South Africa

[e] Department of Civil and Environmental Engineering, Waseda University, Shinjuku, Tokyo 169-8555, Japan

ARTICLE INFO

Article history:
Received 21 October 2025
Revised 9 February 2026
Accepted 13 February 2026

Handling Editor: Sanzhong Li

Keywords:
AHP
Groundwater potential zones
GIS and remote sensing
Thematic layers
Weighted overlay
Puntland
Somalia

ABSTRACT

Mapping groundwater potential zones in a semi-arid region is crucial for sustainable water management. This study used remote sensing and GIS-based AHP to identify groundwater potential zones in the semi-arid district of Garowe, Puntland, Somalia. Nine thematic layers related to groundwater influencing factors were generated using both conventional and satellite-based data. These include rainfall, geology, slope, lineament density, soil, land use/land cover, drainage density, and the normalized vegetation index elevation. Saaty scale values for the thematic layers and their classes were determined based on expert opinions and the literature. Thematic maps were integrated according to their weights and rates to generate a potential zone map through ArcGIS's weighted overlay analysis (WOA) function. The WOA categorizes potential groundwater zones into five levels: abysmal (12.83%, 1116.8 km²), poor (23.77%, 2069.9 km²), good (27.48%, 2383.5 km²), perfect (28.11%, 2446.9 km²), and excellent (7.87%, 685.16 km²). The validation of these zones was conducted using 50 pre-existing data points from boreholes, hand-dug wells, and springs, with the accuracy evaluation performed via the kappa coefficient error matrix. The precise assessment and kappa statistics produced values of 80% and 74%, respectively, confirming the study's reliability. The groundwater potential zone (GWPZ) map was developed as a comprehensive geological tool to support effective groundwater planning and management, particularly during periods of scarcity.

1. Introduction

Groundwater is the most important source of freshwater worldwide. (Sutradhar et al., 2021a). It functions as a reliable source of water for drinking, agriculture, and industry, offering several advantages over surface water, including broader accessibility, greater durability under dry conditions, and higher production potential. (Senanayake et al., 2016; Alshehri et al., 2024; Debela et al., 2025a). Groundwater occurs in the saturated zone, which varies in thickness and depth, under the Earth's surface. Fractures and voids existing in the rocks and unconsolidated materials provide a substantial subterranean reservoir in which a portion of the precipitation is retained (Subramani and Kamaraj, 2024; Subramani et al., 2024). >97% of Earth's water is found in the oceans. The remaining 3% is conserved as freshwater in lakes, glaciers, ice caps, soil and subsoil formations, the atmosphere, and the bodies of biotic organisms. Groundwater constitutes about 30% of the world's freshwater resources and serves as a crucial source of drinking water (Verma and Patel, 2021; Tesfa and Sewnet, 2025).

Climate change, population growth, and urbanization pose a significant threat to many countries, with the most pressing need affecting those already experiencing water scarcity (Kumar et al., 2016a). One potential solution to this issue is to utilize groundwater, which is one of the most valuable natural resources in terms of ecological diversity, economic development, and human health

* Corresponding author at: Puntland State University, College of Engineering and Technology, Department of Water Resource Management, Garowe, Puntland, Somalia.

E-mail address: a.moha1010@gmail.com (A.M. Ismail).

https://doi.org/10.1016/j.geogeo.2026.100521

(Nigussie et al., 2019a). In Sub-Saharan Africa, many cities, particularly in arid and semi-arid regions, depend on groundwater as their primary water supply (Abdullahi et al., 2023a). Therefore, it is essential to develop a comprehensive understanding of groundwater systems across both temporal and spatial dimensions. The World Bank estimates that only 52% of the Somali population has access to a fundamental water supply, with 28% in rural areas and 83% in urban regions (Hassan et al., 2021). In northeast Somalia, characterized by poor and unpredictable rainfall patterns, groundwater is the main source of water supply. The Garowe district, situated in northeast Somalia within the Nugal region, is characterized as semi-arid, with groundwater serving as its primary water source. In this area, groundwater provides approximately 90% of the total annual water supply for agriculture, domestic use, and industry (Hassan and Danert, 2021). Water scarcity in Garowe is due to a lack of surface water resources, rapid population growth, poor, water management strategies, and a lack of data on groundwater sources.

In recent decades, the increasing demand for groundwater across various industries has precipitated a sustained crisis, making it insufficient to satisfy the requirements of a growing population (Araya et al., 2023a). The rising demand underscores the urgent need for strategic management and rehabilitation efforts to facilitate sustainable use and support longer-term developmental goals. (Adiat et al., 2012; Chowdary et al., 2013). Groundwater distribution and availability are determined by considering both local hydrogeological and geological conditions. The most important controlling parameters, including lithology, landforms, lineaments, soil type, land use and land cover (LULC), slope, rainfall intensity, quantity, and infiltration rates, significantly influence groundwater occurrence and flow (Athick et al., 2019a, 2019b; Ndhlovu and Woyessa, 2021). Identification of groundwater potential zones (GWPZs) is crucial for the effective management, development, and allocation of water resources for irrigation, industry, domestic use, and other purposes. Various methods and technologies can be employed to delineate GWPZs and their corresponding characteristics. In recent years, remote sensing (RS) and geographic information systems (GIS) have been widely used along with analytical hierarchy process (AHP) to determine and delineate the area of prospective groundwater zones (Adiat et al., 2012; Nigussie et al., 2019b; Ndhlovu and Woyessa, 2021; Upadhyay et al., 2023; Diriba et al., 2024). Remote sensing offers reliable, economical, temporal, and spectral data over extensive and inaccessible regions (Debela et al., 2025b). Timely mapping and surveillance of the quantity and yearly extraction rates of groundwater resources are essential for attaining sustainable groundwater management. Previously, the most common method of groundwater mapping involved implementing field surveys, supported by geomorphic interpretation, expert knowledge, and additional data processing. However, these techniques are expensive, time-consuming, and labor intensive.

Remote sensing and geospatial data analysis provide an enhanced method for mapping groundwater resources, particularly regarding the pressing need for comprehensive data and evaluations of groundwater conditions (Nigussie et al., 2019b). Thus, remote sensing has emerged as an effective technique for evaluating, monitoring, and preserving groundwater resources (Sreedevi et al., 2015; Balasubramani, 2018). Multiple thematic layers derived from satellite images, for instance, LULC, provide rapid and primary baseline indications on groundwater movement and determining variables for availability (Ban et al., 2015; Gómez et al., 2016). Additionally, rational conditions may also be overlaid on the maps of soils, geology, slope, drainage, and climatic data to delineate groundwater potential areas in a GIS setting (Sutradhar et al., 2021b). Precipitation is the dominant control of an area's groundwater potential, as it is the principal source of water in the hydrological cycle (Ibrahim-Bathis and Ahmed, 2016a). Besides precipitation, the presence and flow of groundwater rely on the geological structure (Nigussie et al., 2019b). Integrating GIS technologies and remote sensing data for investigating groundwater in areas with limited water supplies conserves both time and financial resources.

This study attempts to provide a comprehensive understanding of GWPZs in the region by integrating various factors that affect groundwater recharge, occurrence, and movement, including slope, LULC, drainage density (DD), soil type, geology, lineament density (LD), normalized difference vegetation index (NDVI), and rainfall, as shown in Table 5. Numerous researchers have shown that the integration of remote sensing, GIS, and the analytical hierarchical process (AHP) successfully identifies GWPZs (Sreedevi et al., 2015; Yeh et al., 2016a; Berhanu and Hatiye, 2020a; Pande et al., 2021). This novel approach significantly favors proper observation and timely decision-making by policymakers and water planners. The AHP approach can provide weights to the factors affecting groundwater potential (Golla et al., 2018; Andualem and Demeke, 2019a; Aju et al., 2021a). Groundwater constitutes the primary source of water supply for domestic consumption, industry, and agriculture in the study area; however, limited studies have been conducted for groundwater exploration (Araya et al., 2023b). At various locations within this study area, boreholes drilled by international partners, local NGOs, and local authorities have yielded very low amounts or have dried up after a short period of use. Such cases are a direct indication of borehole drilling without adequate consideration of the surface and subsurface properties determining their occurrences. Therefore, to meet the needs of a rapidly increasing population and urbanization, each nation must examine the possibility of recoverable groundwater deposits through the application of efficient technological methods. The Garowe district lacks research in GWPZs, despite employing labor-intensive approaches such as hydrogeology and seismic analysis. Thus, geospatial methods and remote sensing data could address the knowledge gap by evaluating the groundwater potential in the study region. Mapping and identifying the GWPZ in Garowe provides an excellent water resource management strategy. Prior to this research, the GWPZs in Garowe city had not been identified. The literature review confirms the lack of research aimed at mapping groundwater potential areas, largely due to access, cost, and transportation challenges. This research paper seeks to address the research gap in the study area by evaluating the groundwater potential zones of the Garowe district and contribute an advanced integrated water resource management approach in the region. The specific objective of this research is to identify the parameters controlling groundwater potential zones, prepare thematic layers/maps, overlay these layers in GIS software, and finally validate the results using available borehole data and past trends in the study area.

2. Material and methods

2.1. Description of the study area

This research was conducted in the Garowe district of Puntland, Somalia, located at latitudes 8°4′40′′–9°5′20′′ N and longitudes 48°0′20′′–49°1′0′′ E (Fig. 1) covering an area of 8702.3 km^2. Garowe city serves as the administrative center of the Puntland State of Somalia and is situated in a region surrounded by rugged terrain and semi-arid landscapes.

The region features a diverse array of physical landscapes, including plains, steep gorges, flat-topped plateaus, and rugged high mountains. Elevation varies from 840 m to 280 m above sea level, gradually decreasing toward the east and northeast, as shown in Fig. 1. In the highly elevated and steep catchment, gravity helps water flow toward the stream channel, while in gently sloping watersheds, water is retained longer, increasing infiltration and groundwater recharge. The drainage pattern is dendritic, with main

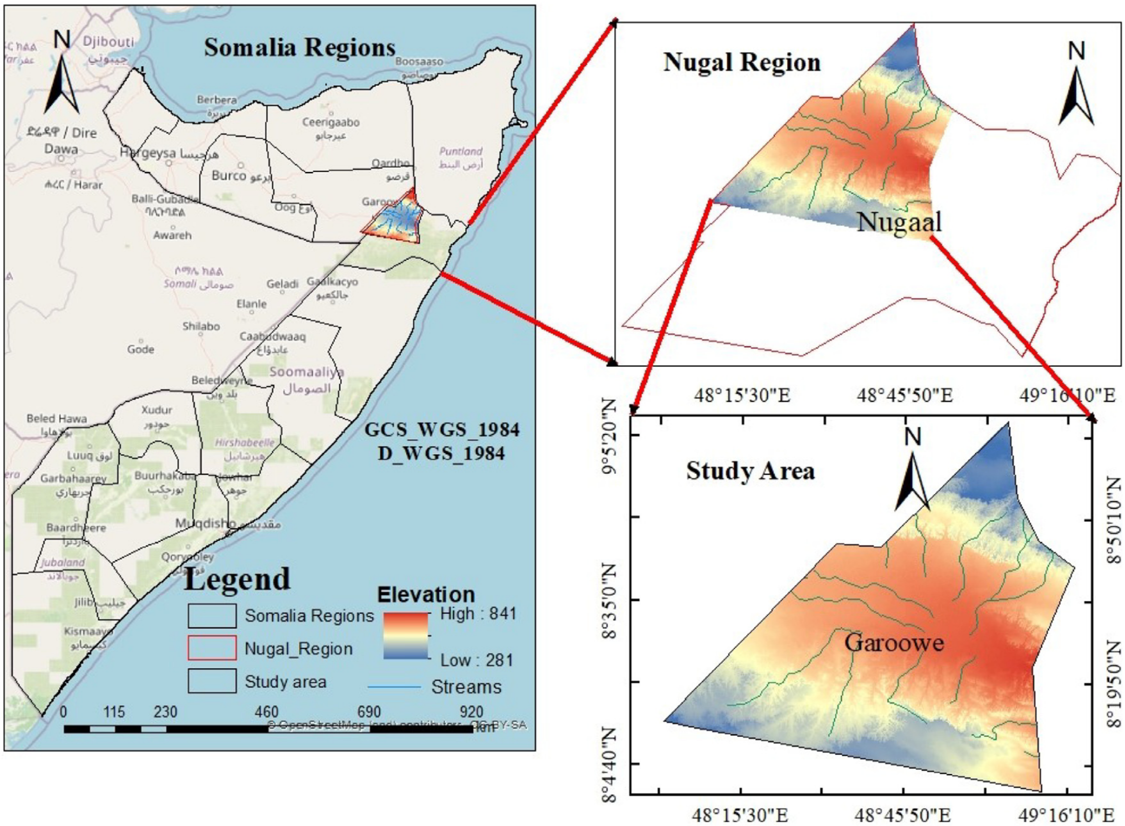

Fig. 1. The location map of the study area.

Table 1
Data sources used in the study.

Data Types	Data Source	Data type and acquisition data	The function of the data	Reference
SRTM DEM (10 m)	USGS	Grid 22/5/2025	SL, DD, and EL, maps	https://earthexplorer.usgs.gov/
Rainfall	CRU TS v. 4.06/	0.5° × 0.5°/2014–2024	Rainfall map	https://crudata.uea.ac.uk/cru/data/hrg/cru_ts_4.06/
Soil data	MOWRE and FAO	Polygon/2023	Soil map	https://storage.googleapis.com/fao-maps-catalog-data/uuid/446ed430-8383-11db-b9b2-000d939bc5d8/resources/DSMW.zip
Landsat 8 OLI/TIRS	USGS	22/5/2025	LULC, LD, and NDVI maps	https://earthexplorer.usgs.gov/
Geological data	USGS and MOWRE	Polygon 1:250,000/2020	Lithology map	https://www.usgs.gov/centers/central-energy-resources-science-center/science/world-geologic-maps

Note: USGS – United States Geological Survey; CRU TS vs. 4.04 – Climatic Research Unit gridded Time Series version 4 data; MOWRE – Ministry of Water Resources and Energy; SL – Slope; DD – Drainage density; EL – Elevation; LULC – land use land cover; NDVI- Normalized Difference vegetation Index; LD – Lineament density.

rivers such as Major Maqarshe and Armalle originating in high-altitude areas and flowing eastward to the Indian Ocean, joining numerous streams along the way. Garowe has a desert climate, with summer days frequently reaching 38 °C—long, hot, and dry. Winters are milder, with daytime temperatures ranging from 20 to 30 °C and cooler nights. Rainfall is generally low, resulting in dry, dusty, and windy conditions, with limited vegetation, including shrubs and acacia trees, which are adapted to an arid environment.

2.2. Data sources

Table 1 lists the data sources. Landsat 8 Operational Land Imager/Thermal Infrared Sensor (OLI/TIRS) data for path 162 and row 052 were downloaded on May 22, 2025, from the US Geological Survey website. These data were used to generate lineament density (LD), normalized difference vegetation index (NDVI), and LULC maps for the study area. Geological data were updated using information from the Ministry of Water Resources and Energy (MOWRE) and used to develop the area's lithological unit. The Shuttle Radar Topography Mission Digital Elevation Model (SRTM DEM) with a spatial resolution of 10 m was obtained from the US Geological Survey website (accessed on May 22, 2025). These data were used to generate slope, drainage density, and elevation maps of the study area. Rainfall data from 2014 to 2024 were obtained from the CRU TS v. 4.06 website, which provides high-resolution gridded data at 0.5° × 0.5° Soil data were obtained from the Ministry of Water and Energy and updated with FAO soil data. These data were used to determine the soil type.

2.3. Research methods

Various criteria were employed to identify groundwater potential zones. Raster maps of the relevant variables were generated using GIS (version 10.8) and Envi (version 5.6) from remote sensing data. These thematic layers included land use/land cover, slope, elevation, NDVI, lineament density, drainage density, soil texture, and geology. Atmospheric and radiometric corrections were applied with the Semi-Automatic Classification Plugin. In GIS, processes such as conversion, interpolation, categorization, reclassification, augmentation, and filtering were used to process the satellite data. Elevation data from the Shuttle Radar Topography Mission Digital Elevation Model (SRTM DEM), with a 10 m × 10 m resolution, improved accuracy in both vertical and horizontal measurements. This data was used to produce an elevation map in ArcGIS. The elevation information was then used to generate slope raster data for each grid cell by calculating the maximum rate of change between neighboring cells. Slope classes were classified using the Slope Spatial Analyzer tool. Drainage density, inferred from the slope data, was calculated to measure the spacing of stream channels, defined as the total stream length per unit area (Sar et al., 2015). The stream order was determined through flow accumulation and flow direction operations in ArcGIS. The drainage lines were assessed by evaluating stream lengths greater than 1000 units ("value > 1000"), and drainage density (km/km²) was calculated as shown in Eq. (1).

$$D_D = \sum_{i=1}^{n} \frac{D_I}{A} \tag{1}$$

where D_i is the total stream length in stream order ith (km), and A is the basin area (km^2). Utilizing PCI Geomatics 2016, the Landsat 8 OLI/TIRS image (path 162, row 52), exhibiting 5% cloud cover, was extracted to compute the lineament density of the study region. In recent years, high-resolution satellite imagery has proven to be an effective technique for mapping groundwater in arid and semi-arid regions. The thematic layer for lineament density (LD) is defined as the cumulative length of all identified lineaments relative to the area of the catchment under consideration(Das, 2019a). The calculation of lineament density was done using Eq. (2).

$$\boldsymbol{L_D} = \sum_{i=1}^{n} \left(\frac{L_i}{A} \right) \tag{2}$$

where L_i is the length of the i^{th} lineament, ΣL_i is the sum length of all lineaments in kilometers, and A is the grid size in square kilometers. Lineament extraction was performed with random lines in various regions based on hillshade analysis. Subsequently, lineaments were extracted using ArcMap 10.8. The manual extraction of lineaments is more dependable than alternative automated techniques (Alshehri and Abdelrahman, 2023). The geological, or lithological, thematic map of the study area was downloaded from USGS and updated with the latest (2015) geological maps of the Garowe district from the Ministry of Water Resources and Energy, Somalia (MOWRE, 2015). The ESRI land cover of Sentinel-2, at a 10-meter resolution, was used to determine the recent (2024) LULC map of the study area. We obtained the soil map of the study area from FAO (2003) data and MOWRE's Somalia soil map (Table 1). A rainfall map of this research was created using the inverse distance weighting (IDW) interpolation approach. The NDVI assesses the greenness of vegetation and serves as a strong indication of temporal changes in vegetation within a specific area. The NDVI layer was created using the Near Infrared and Red bands in the Raster Calculator of ArcGIS 10.8 Eq. (3).

$$NDVI = \frac{NIR - RED}{NIR + RED} \tag{3}$$

where NIR represents the near-infrared band, whereas RED signifies the red band in the reflectance values of the electromagnetic spectrum. Finally, the delineation of the groundwater potential zone involved converting all data layers into raster format, maintaining a uniform spatial resolution of 10 m × 10 m. The relative importance of each element influencing groundwater potential was assessed by a pairwise comparison of all features. Each map was categorized using computed weights. The weighted overlay module in ArcGIS 10.8 was used to create a groundwater potential map by integrating all thematic layers. The groundwater potential zones identified through GIS and RS techniques were assessed against existing ground data from boreholes, springs, and hand-dug wells to confirm the validity of the qualitative results. This enhanced confidence in the application of qualitative results derived from GIS and RS analysis. The overall framework for data processing and analysis is illustrated in Fig. 2.

2.4. Multi-criteria decision-making methods

A multi-criteria decision-making method is employed to evaluate groundwater potential. It includes multi-influencing factor (MIF), analytical hierarchy process (AHP), fuzzy logic (FL), frequency ratio (FR), certainty factor (CF), weights-of-evidence (WOE), and index models (IM). In this study, the analytic hierarchy process (AHP) was used to identify groundwater potential zones (Murmu et al., 2019; Owolabi et al., 2020; Sahoo et al., 2024). The AHP method is a highly efficient decision-making tool, with consistently dependable results (Andualem and Demeke, 2019b). It minimizes complex judgments into a series of pairwise comparisons and then integrates the results. Moreover, AHP serves as an effective instrument for assessing the consistency ratio of results to mitigate biases in the decision-making process (Saaty, 1990).

2.5. The analytical hierarchy process (AHP)

The analytic hierarchy process (AHP) is an effective decision-making approach for addressing complex problems. It is used to identify potential solutions while analyzing multi-criteria decision-making situations. This method provides the assessment of the relevance of various characteristics through pairwise comparisons, allowing the AHP analysis to perform a significance test on the features (Abdullahi et al., 2023b). Saaty proposed mathematical equations to determine the optimal solution in a multi-criteria analysis (Saaty, 1990).

In this study, we used the mathematical principles of AHP and related computational methods to create a matrix that expresses the relative values of a set of attributes. The approach consists of four steps: problem modeling and hierarchical structure formation, pairwise comparison, weight evaluation, and weight aggregation. The current study employed AHP to determine the weights of factors based on weight assignments and normalization, considering the relative contributions of various themes to groundwater occurrence (Kumar et al., 2016b). AHP employs a preference matrix to assess relevant criteria and consolidates the weights to ascertain the requisite weights for various criterion map layers. To use Saaty's scale of relative significance, the first step is to construct a pairwise comparison matrix (PCM), as described by Saaty. Table 2 illustrates the normalized weights following the importance ranking of each layer. Weights were allocated to the critical layers using the pairwise comparison technique.

A senior hydrogeologist, a hydrologist from the Ministry of Water Resources and Energy (WOWRE), the Puntland Water Development Agency (PWDA), and the local authority office were invited to establish the relative significance of indicators using Saaty's scale values (Table 2) for the construction of the pairwise comparison matrices. Furthermore, we meticulously examined several previous works to incorporate the perspectives of hydrologists and researchers; therefore, we constructed pairwise comparison matrices with precision and assessed the significance of characteristics influencing groundwater occurrence. Satty's nine-point significance scale (Saaty, 1990), facilitated the derivation of the pairwise comparison matrix. The relative significance values are assessed on a scale of 1 to 9 (Table 2). Saaty (1990), proposed a nine-point scale

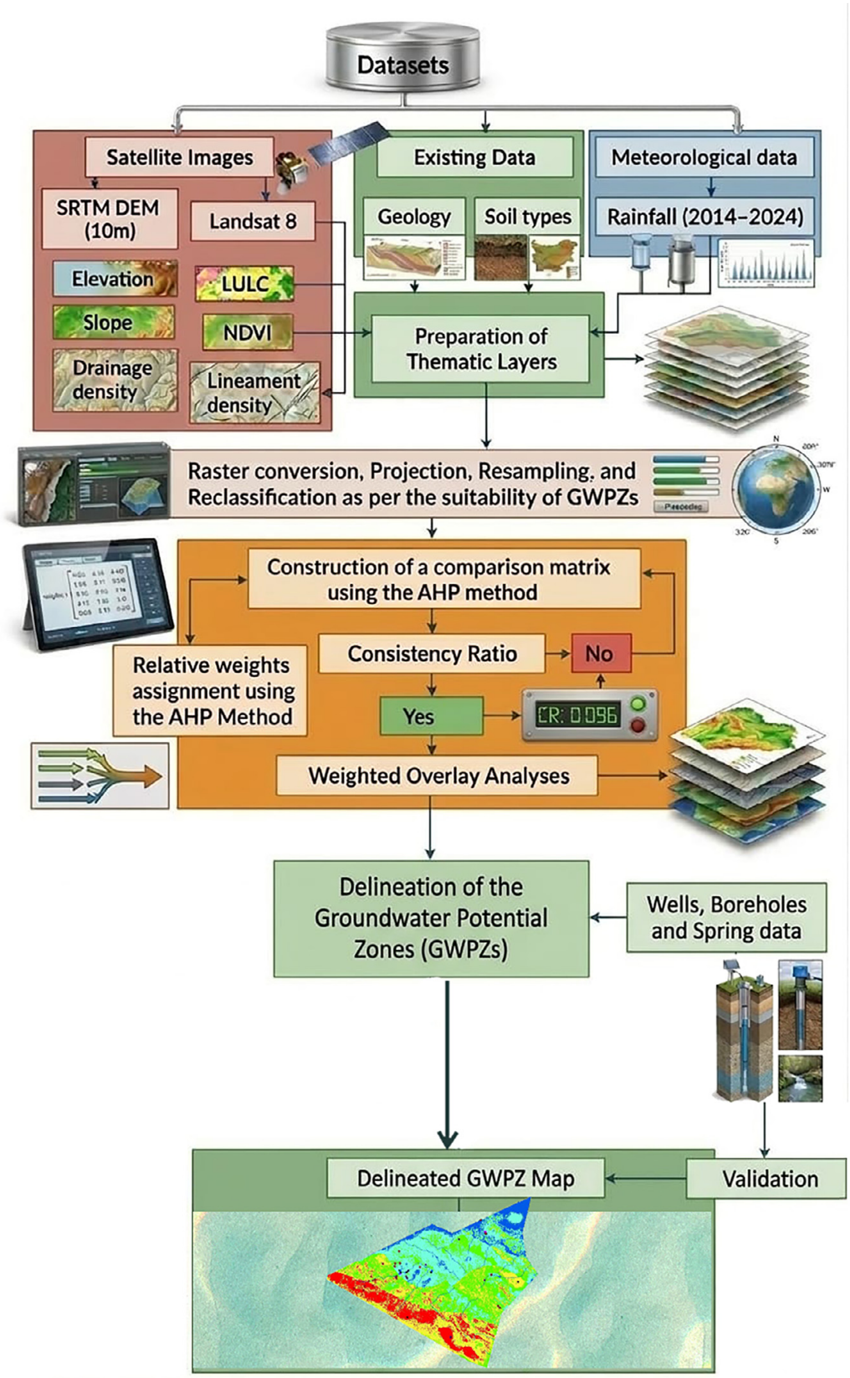

Fig. 2. Methodological framework for the research.

Table 2
Saaty's relative significance scale.

Scale	Definition	Explanation
1	Equal importance	Two elements contribute equally to the objective
3	Moderate importance	Experience and judgment slightly favor one element over another
5	Strong Importance	Experience and judgment strongly favor one element over another
7	Extreme importance	One element is favored very strongly over another; its dominance is demonstrated in practice
9	Extreme importance	The evidence favoring one element over another is of the highest possible order of affirmation
2, 4, 6, and 8		Intermediate numbers

Source: (Saaty, 1990).

Table 3
Satty's scale of relative importance and RI.

Number (N)	1	2	3	4	5	6	7	8	9
Randomized Index (RI)	0	0	0.58	0.9	1.12	1.24	1.32	1.41	1.45

Source: (Saaty, 1990).

ranging from 1.1 to 1.9 to assess options that indicate slight variations (Table 3). Each element was evaluated using a scale based on actual issues, taking into account the significance of each criterion in the occurrence of groundwater. Finally, a pairwise comparison matrix ($n \times n$) was generated based on the input factors (Table 6). Each entry indicates the influence of the row-relative on the column-factor. We compare the elements at each level of the matrix in pairs to determine their significance to the elements at the next higher level. Starting at the top of the hierarchy and proceeding downward, the pairwise comparison square matrices were constructed so that all components inside the matrix are positive, as shown in Eq. (4).

$$A = \left[a_{ij}\right] = \begin{bmatrix} a_{11} & a_{21} & .. & a_{1n} \\ a_{12} & a_{22} & .. & a_{2n} \\ \dots & \dots & .. & .. \\ a_{1n} & a_{1n} & .. & a_{nn} \end{bmatrix} \tag{4}$$

where $[a_{ij}] > 0$. The diagonal elements of the square matrix equal one, because identical factors possess equivalent weight, as shown in Eq. (4). Therefore, the upper and lower triangular matrices must be constructed by comparing the components with one another. Eq. (5), as shown below, calculates the lower triangular matrix.

$$a_{ij} = \frac{1}{a_{ij}} \tag{5}$$

Subsequently, the matrix is summed, and each element is divided by the sum of its column to obtain the normalized relative weight, as shown in Eq. (6) and Table 7

$$w = \frac{a_{il}}{\sum_{i=1}^{n} a_{ij}} \tag{6}$$

where n stands for the number of elements in the column, and W is the normalized weight. Finally, the weights of the pairwise matrix are computed by averaging the normalized relative weights in each row for every class, adjusted by a factor corresponding to the higher hierarchy as described in Eq. (7).

$$W = \sum_{j=1}^{n} \frac{(w)ij}{n} \tag{7}$$

2.6. Calculation of the CI and CR

The accuracy of groundwater zonation was evaluated using the consistency index (CI) and consistency ratio (CR). The AHP consistency ratio approach was used to assess the consistency of the weighted criterion layers. Saaty (Saaty, 1990) proposed the consistency index (CI) as a measure of variation or degree of consistency, using Eq. (8).

$$CL = \frac{\lambda_{\max} - N}{N - 1} \tag{8}$$

where $\lambda_{\max}$ is the maximum eigenvalue, and N is the order of the comparison matrix. Eq. (9) is used to determine $\lambda_{\max}$ using weighted sum and priority:

$$\lambda_{\max} = \left(\frac{\sum\left(Weighted\ sum\ or\ priority\right)}{N}\right) \tag{9}$$

where N is the order of the comparison matrix. Efficiency requirements are assessed using the consistency ratio (CR) in Eq. (10)

$$C_R = \frac{C_I}{R_i} \tag{10}$$

where RI represents the random consistency indices. Saaty (Saaty, 1990). provided the RI, as shown in Table 3. When CR > 0.1, there is evidence of an error in the ranking of the criteria/factors. As such, it needs to recalculate the relative importance of the elements at stake. When CR is below 0.1, the overall weight assigned to each element is suitable for decision-making.

2.7. Weighted overlay analysis (WOA)

A weighted overlay GIS model was used to identify suitable prospective areas for groundwater potential. The groundwater prospect zones were assessed using the groundwater potential index (GWPI), which was derived from the integration of all thematic levels that affect groundwater. The 'weighted overlay analysis' tool was used to calculate groundwater potential index values using Eq. (11), provided by Malczewski Jacek (1999). The GWPI values were used to identify whether an area is excellent, very good, good, poor, or very poor with respect to groundwater potential (Andualem and Demeke, 2019b; Godif and Manjunatha, 2023; Mohammed et al., 2025).

$$GWPZ = \sum_{j=1}^{m}\sum_{i=1}^{n}\left(W_j * X_i\right) \tag{11}$$

W_j denotes the normalized weight of the jth theme layer, X_i represents the rate value of each class on the jth layer, m signifies the total number of thematic layers, and n represents the total number of classes within each thematic layer.

2.8. Validation process

The delineated groundwater potential zones, obtained using GIS and RS approaches, were compared with existing ground data from boreholes, springs, and hand-dug wells in the study area to verify the precision of the analysis. This would enhance trust in the use of qualitative data derived from GIS and RS analysis. The precision of the designated zones is evaluated based on the total quantity of validation data and the total quantity of disagreement data. Eq. (12) was used to calculate the validation process of the groundwater potential zones of this study

$$GWPZ = \left(\frac{Total\ no.\ of\ validation\ data - Total\ no.\ of\ disagreement\ data}{Total\ no.\ of\ validation\ data}\right) \times 100\% \tag{12}$$

3. Results and discussion

3.1. Slope

Slope refers to the rate of elevation change and is an essential factor in determining groundwater potential zones (Das, 2019b). Groundwater recharge is directly influenced by slope, which describes the degree of steepness or elevation variation between two

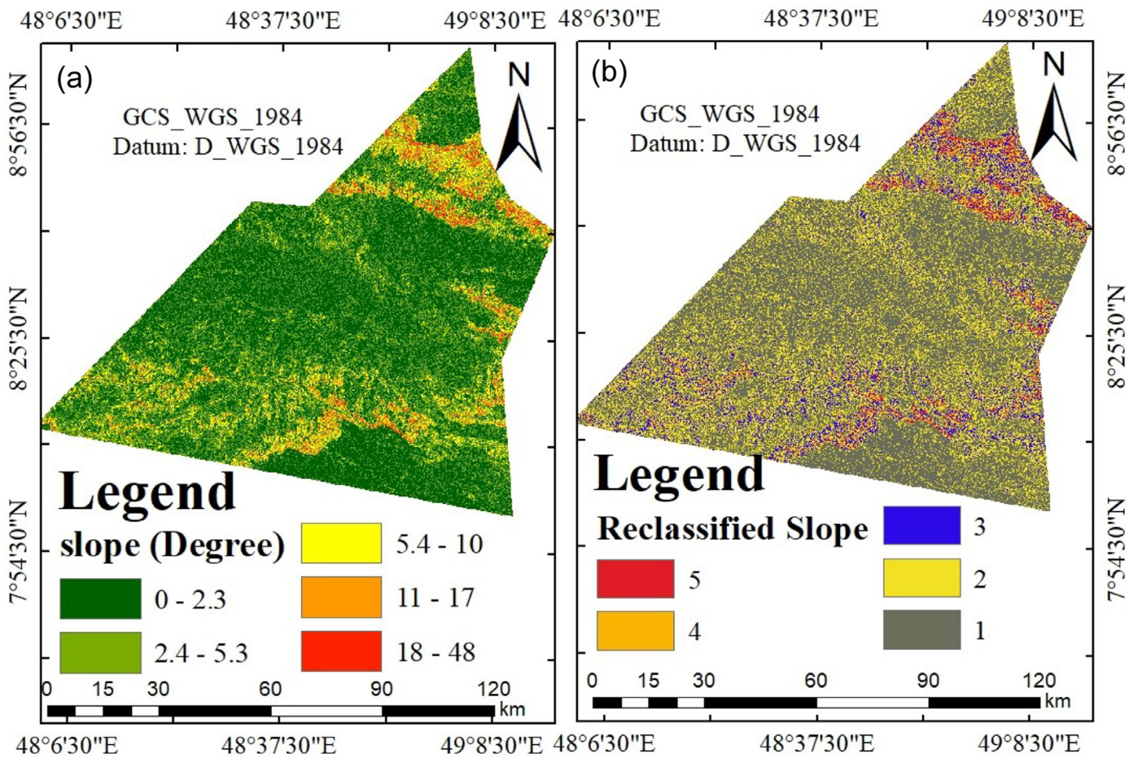

Fig. 3. Maps showing (a) slope (degree) and (b) reclassified slope.

points. High-slope areas are unsuitable for groundwater recharge, resulting in increased runoff and soil erosion. In contrast, a gentle and nearly flat slope allows for gradual water flow, providing sufficient time for infiltration into the soil (Ibrahim-Bathis and Ahmed, 2016b). This study utilized the spatial analyst tools in ArcGIS version 10.8 to generate the slope map (Fig. 3) from the digital elevation model (DEM) data. The slope map of the study area is categorized into five classes using the natural breaks (Jenks) classification method: (0–2.3°) flat areas, (2.4–5.3°) gentle areas, (5.4–10°) moderate areas, (11–17°) high areas, and (18–48°) steep areas, respectively, as shown in (Fig. 3a). The slope was divided into five categories to determine groundwater potential zones, as shown in Table 5 and illustrated in Fig. 3b.

The Jenks classification thresholds method enables to decrease the variation within class whereas maximizing between-class variance (Ndhlovu and Woyessa 2021; Upadhyay et al. 2023). Approximately 85% of this study encompasses flat to gently sloping terrain, allowing greater water infiltration than runoff. The slope reclassification map indicates a reciprocal association between slope and groundwater production (Yeh et al., 2016a), with the gentlest slope class (0–2.3) assigned the maximum weight of "5", whereas the steepest slope class (17–48) received the lowest weight value of "1" (Table 5).

3.2. Elevation

The elevation of the study area represents the terrain's roughness, and it is important for identifying potential groundwater zones. Low-elevation shallow areas often retain water for extended periods, leading to increased water percolation. Areas with higher elevations have elevated outflow and less infiltration. The research region's elevation ranges from 280 to 840 m above mean sea level, as shown in Fig. 4a. Elevated altitudes are observed in the southern and western parts of the research area. In contrast, the eastern and northern parts had relatively lower altitudes (Fig. 4a). The elevation map was determined using the SRTM DEM, which has a spatial resolution of 10 m, due to its precise vertical and horizontal accuracy (Deepika et al., 2013). Elevation is classified into five categories based on altitude from mean sea level (MSL): 280–400 m, 410–490 m, 500–580 m, 590–690 m, and 700–840 m within a GIS environment. The elevation data were then reclassified into five classes based on the suitability ranking of groundwater occurrences using the reclassification tool in ArcGIS, Fig. 4b, and Table 5.

The suitability of groundwater decreased with increased elevation. The lower topography retains more water than the elevated area. Therefore, the maximum weight of 5 was assigned to low-elevation regions, while the minimum weight of 1 was assigned to high-elevation areas, as seen in the elevation reclassification map, Fig. 4b, and Table 5.

3.3. Land use land cover (LULC)

Land use refers to human activities on land for various purposes, whereas land cover refers to the characteristics resulting from land transformation. Remote sensing data primarily gather information on the land surface, which is crucial for determining land use information. Land cover dynamics, climate change, and the extreme demand for a significantly increasing population are worldwide issues with profound ramifications for human livelihood and systems (Zewdie and Tesfa, 2023). The land use and land cover of the area have a great effect on both surface and subsurface conditions, including soil erosion, soil moisture, soil fertility, surface runoff, infiltration, sedimentation, evapotranspiration, and other entities (Diriba et al., 2024). Vegetated surfaces, such as forests and agricultural land, retain water in plant roots, where urban and rocky terrains influence groundwater recharge by enhancing runoff during precipitation (Berhanu and Hatiye, 2020b). Therefore, exploring the characteristics of the research area, LULC, is essential for determining groundwater potential assessments. The LULC significantly influences several hydrologic processes, includ-

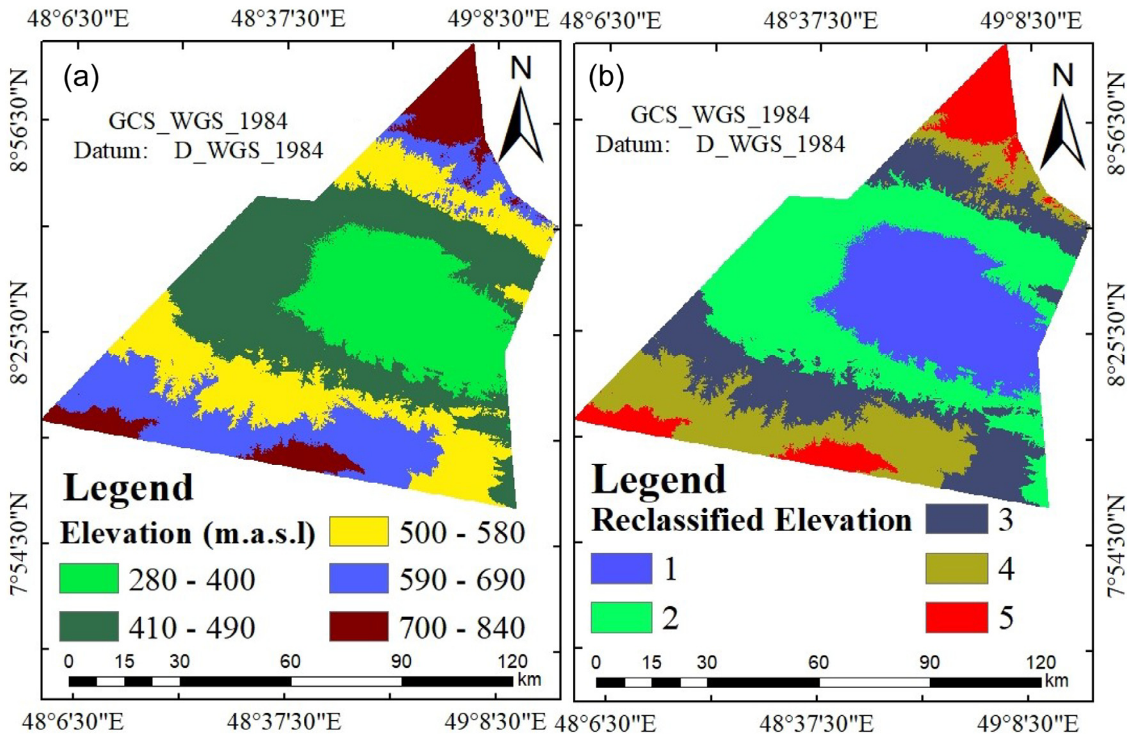

Fig. 4. Maps showing (a) Elevation and (b) reclassified elevation.

Table 4
Land-use/land-cover types and coverage of the study area.

No.	LU/LC Class	Area (km^2)	Percentage (%)
1	Bare ground	1044.57	11.99
2	Built area	9.96	0.11
3	Crops	2.54	0.03
4	Rangeland	7655.93	87.86
5	Trees	0.78	0.01
6	Water	0.01	0

ing changing surface runoff dynamics, groundwater recharge, evapotranspiration, transpiration, infiltration, evaporation, and interception. Many watersheds are experiencing changes in land use and cover due to population growth and other human-caused factors (Li et al., 2018; Riley et al., 2019; Berhanu and Hatiye, 2020a). The LULC map of this study has been generated and reclassified using Landsat 8 OLI/TIRS and the maximum-likelihood algorithm. This analysis identified six key land-use and land-cover units, including rangelands, bare ground, built areas, crops, forests, and water, as indicated in Fig. 5a and Table 4. The LULC map of this study has been generated and reclassified using Landsat 8 OLI/TIRS and the maximum-likelihood algorithm Fig. 5b 99.85% of the LULC of this study encompasses rangelands and bare lands, while the remaining 0.15% encompasses other land covers, specifically settlements, crops, and forests or trees, accounting for 0.11%, 0.03%, and 0.01% of the total area, respectively (Fig. 5 and Table 4).

Built and barren surfaces have less potential for retaining groundwater compared to vegetated areas, such as those covered by crops and forests (Berhanu and Hatiye 2020a, 2020b). The built-up area constituted the land-use category with the least weight compared to the other classifications. On the other hand, forests have the highest rating due to decreased runoff, which increases the likelihood of groundwater recharge. Therefore, the maximum weight of 5 was allocated to forest regions, while the built area received the lowest score of 1, as seen in Table 5.

3.4. Rainfall

Precipitation is the main source of groundwater recharge, as it strongly influences the infiltration, hydrological cycle, and groundwater potential (Guddeti et al., 2024). It is designated as the main storage of groundwater and governs its variations (Andualem and Demeke, 2019b). Understanding the intensity and duration of precipitation may provide the estimation and prediction of its impacts on runoff, infiltration, and groundwater recharge. The intensity and duration of precipitation have a substantial influence on groundwater recharge. Short and intense precipitation causes less infiltration and increased surface runoff, whereas prolonged, less intense rainfall increases infiltration rate relative to runoff (Ibrahim-Bathis and Ahmed, 2016a). The study area experiences a peculiar precipitation regime characteristic of its semi-arid state. The primary rainy season, the Gu, occurs between April and June, and the study area receives its yearly precipitation, averaging approximately 76 to 100 mm.

The second rainy season, the Deyr, occurs between October and December and is of lower intensity. A rainfall map was generated in ArcGIS using the Inverse Distance Weighting (IDW) interpolation technique on data sourced from CRU TS (https://crudata.uea.ac.uk/cru/data/hrg/), updated with data obtained from rain gauge stations. The technique used deterministic approaches, whereby IDW calculates cell values by averaging the values of nearby sample points. The maximum precipitation occurred in the southern and eastern regions of the study area, whereas the minimum was recorded in the western and northern regions, as illustrated in Fig. 6a. The rainfall data were grouped into five categories based on the suitability ranking for groundwater occurrences using the reclass tool in ArcGIS (Fig. 6b and Table 5. Regions with increased precipitation have elevated recharge rates compared to regions with less rainfall. The region with the maximum precipitation was assigned a score of "5" while the region with minimal rainfall received the lowest rating of "1" (Table 5).

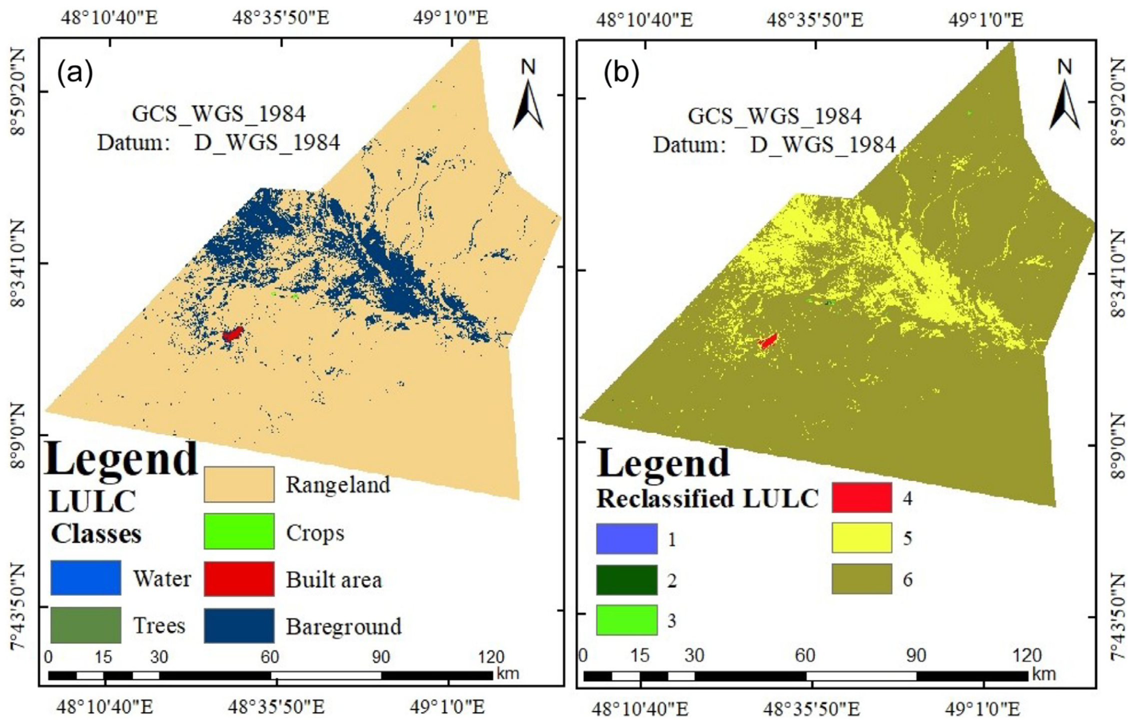

Fig. 5. Maps showing: (a) LU/LC and (b) reclassified LU/LC.

Table 5
Reclassification and rating of layer suitability for the identification of groundwater potential zones.

Thematic Layers	Description	Reclassification values and layer suitability for identification of groundwater potential zones					Source
	Ranking Classification	1 Very poor	2 Poor	3 Moderate	4 High	5 Very High	
Elevation	Mean above sea level (m)	840 –700	690–590	580–500	490–410	400–280	Ally et al., 2024b; Rahim et al., 2025; Tesfa and Sewnet, 2025
	Category	Ver Low	Low	Moderate	High	Very High	
Slope	Degree	>48	17–11	10–5.4	5.3–2.4	2.3–0	Rather and Andrabi, 2012
	Category	Very steep	Steep	Moderate	Gentle	Flat	
Drainage density	Value (km/km^2)	1.4–1.2	1.1–0.83	0.82–0.56	0.55–0.29	0.004–0.28	Nigussie et al., 2019a; Alshehri and Abdelrahman, 2023; Diriba et al., 2024;
	Category	Very Low	Low	Moderate	High	Very High	Berhanu and Hatiye 2020a
Geological units	Types of Geological Units	0	0	Tertiary	Holocene		Lavanya and Muthukumar, 2024
Soil texture	Soil types	0	Lithosols	Gypsic Yermosols	Calcic Yermosols	Calcic Xerosols	Ibrahim-Bathis and Ahmed, 2016a
	Category	0	Low	Moderate	High	Very High	
Rainfall	Value (mm)	76–82	83–88	89–92	94–96	97–100	
Lineament density	Density (km/km^2)	1.6–1.3	1.2–0.94	0.93–0.63	0.62–0.32	0.31–0	Sar et al., 2015; Sahoo et al., 2024; Mishra and Singh, 2019
	Category	Very High	High	Moderate	Low	Very Low	
LU/LC	Type	Built area	Bare land	Rangeland	Crops	trees	Alshehri and Abdelrahman, 2023; Sahoo et al., 2024
	Category	Very Low	Low	Moderate	High	Very High	
NDVI	Degree	−0.02–0.075	0.075–0.088	0.088–0.1	0.088–0.169	0.19–0.440	Alshehri and Abdelrahman, 2023
	Category	Very Low	Low	Moderate	High	Very High	

3.5. Drainage density (DD)

Drainage density (DD) refers to the closeness of stream channel spacing and is defined as the ratio of the cumulative length of stream segments of all orders to a unit area (Berhanu and Hatiye, 2020b). Drainage density was calculated using Eq. (1). It is an essential variable in evaluating groundwater recharge and the availability of groundwater. It provides important details on the hydrological landscape, including infiltration and the underlying lithology (Godif and Manjunatha, 2023; Khushi et al., 2023; Ally et al., 2024a). Higher drainage density promotes increased runoff via the fragmented channels, thereby decreasing the potential for ground infiltration and subsequent percolation. On the other hand, areas with low drainage density provide less surface runoff, resulting in increased infiltration and opportunities for groundwater recharging (Jenifer and Jha, 2017; Thomas and Duraisamy, 2018). Drainage density is inversely related to permeability, significantly influencing runoff dispersion and infiltration levels. The Arc Hydro tool version 10.8 for ArcGIS retrieves and defines drainage networks using the Digital Elevation Model (DEM). In this research area, the DD varies from 0 to 1.4 km/km^2 and is categorized into five classifications: 0.004–0.28, 0.29–0.55, 0.56–

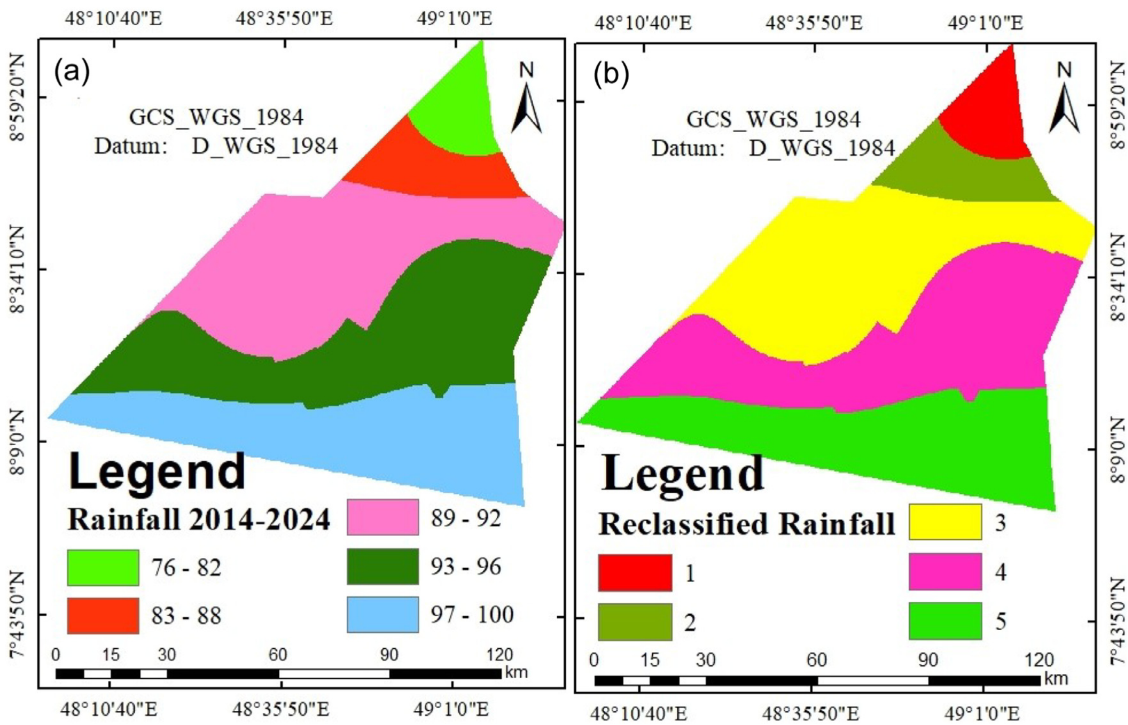

Fig. 6. Maps showing (a) rainfall and (b) reclassified rainfall.

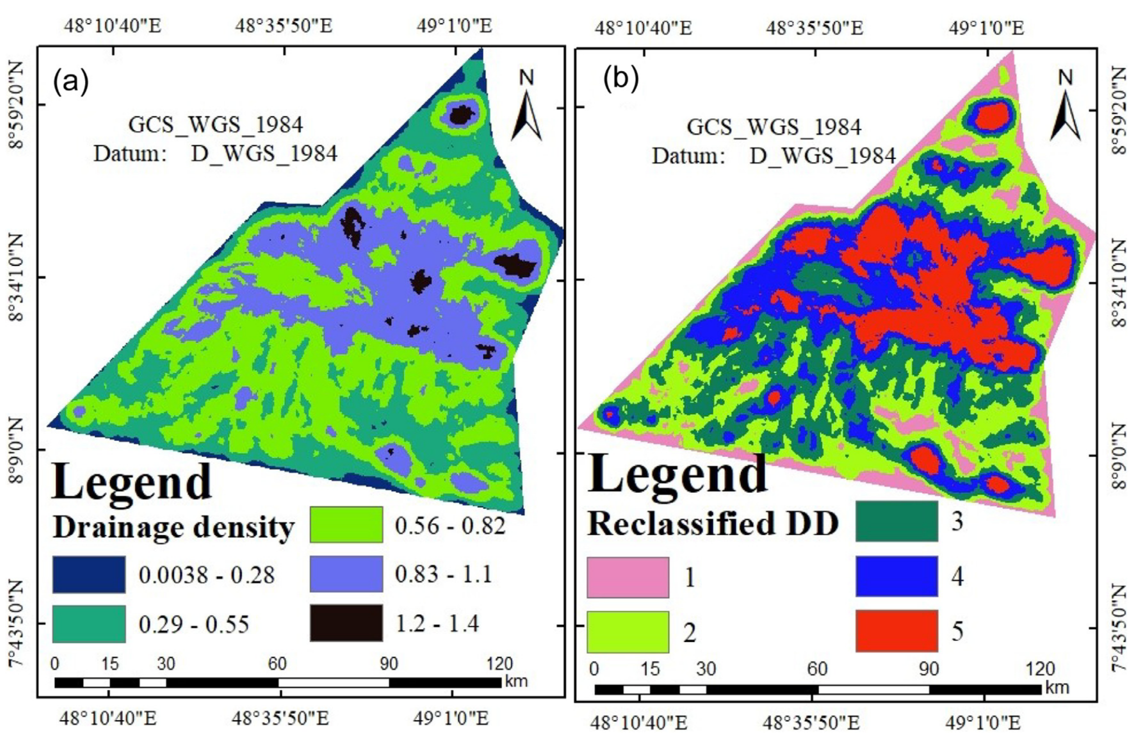

Fig. 7. Maps showing (a) drainage density and (b) reclassified drainage density.

0.82, 0.83–1.1, and 1.2–1.4 km/km², as indicated in Fig. 7a and Table 5. The drainage density in the study area has been divided to delineate groundwater potential zones (Fig. 7b and Table 5). Regions exhibiting high drainage density (1.1 to 1.4 km/km²) are considered unsuitable for groundwater presence, receiving a score of 1, whereas areas with low drainage density (0–0.28 km/km²) are categorized as extremely favorable for groundwater occurrence, assigning a score of 5 (Table 5).

3.6. Lineament density (LD)

The presence of groundwater in rock formations is mainly affected by fractures and lineaments, as well as the pores within sedimentary strata (Debela et al., 2025b). Lineaments signify areas with cracked and faulted features, which experience increased secondary porosity and permeability. Lineaments directly affect groundwater transport, as they signify the naturally occurring per-

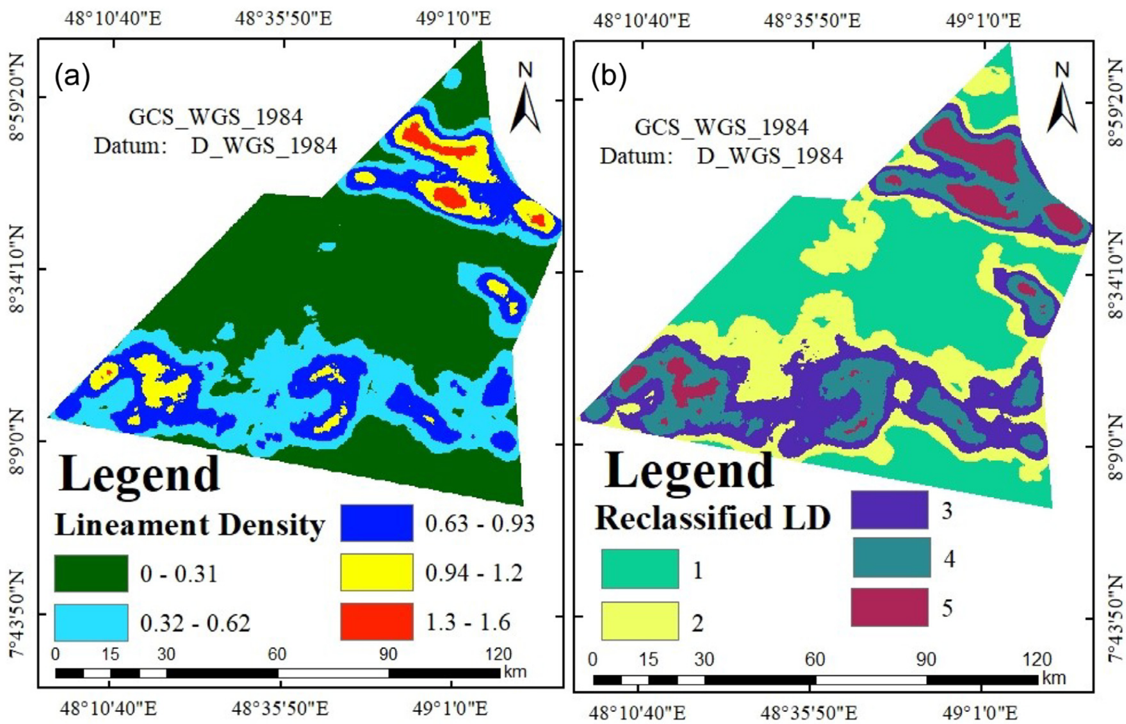

Fig. 8. Maps showing (a) lineament and (b) reclassified lineament density.

meable zones within hard rock formations. The lineament density in this study was determined using Eq. (2), which is provided in the methodology section. Higher weights are allocated to areas with higher LD values due to the positive association between groundwater potential (GWP) and LD (Rasool et al., 2020). The study characterizes lineaments as linear, rectilinear, and curved structures of tectonic origin (Fig. 8). The spatial resolution of a satellite image is essential for detecting lineaments; thus, a processed DEM was used to extract lineaments. The features were manually retrieved by on-screen digitization in ArcGIS using a hill shade derived from DEM data. Many lineaments are aligned in southeast to northeast (SE-NE) orientation, like the regional MER alignment. The lineament map is then transformed into zones of varying lineament density, ranging from 0 to 1.6 km/km^2 (Fig. 8a). Elevated lineament densities were observed in the southeastern region, whereas decreased densities have been identified in the western and central areas of the study area. We assign a higher score to areas with elevated lineament density as potential groundwater zones. Lineament density is categorized into five groups and prioritized based on their appropriateness for groundwater accumulation (Fig. 8b and Table 5).

3.7. Normalized vegetation index (NDVI)

The NDVI is used to evaluate the groundwater potential in specific areas by estimating the level of health and density of vegetation cover. The NDVI is a commonly used statistic for assessing vegetation cover, as it serves as an indicator of plant growth and production. Due to the enhanced surface storage component, plants can capture rainwater on their leaves and branches, thereby increasing evapotranspiration and extending the duration required for soil recharging. The amount of solar radiation reflected by the vegetation cover is correlated with wavelength, chlorophyll concentration, leaf internal structures, and plant moisture content. Radar backscattering is used to assess surface roughness and soil moisture content (He et al., 2014; Snapir et al., 2014; Mansaray et al., 2017). The present study used the normalized difference vegetation index (NDVI) obtained from Landsat 8 imagery to create the NDVI map of the study areas, as illustrated in Fig. 9a. The NDVI was calculated utilizing Eq. (3) as described in the methodology section. This study produced five NDVI classes (Fig. 9b and Table 5). The lowest NDVI values (−0.046 to 0.089) were observed in large parts of the study area, including built areas, and received the lowest score 1, while the highest normalized difference vegetation index (NDVI) values (0.18 to 0.43) were assigned the highest score 5, as shown in Table 5.

3.8. Geology

Geology plays a crucial role in determining the occurrence of groundwater (Aju et al., 2021b). The permeability and porosity of various rock types, including transitional alkaline and sub-alkaline basalts and rhyolites, affect runoff and infiltration rates (Yeh et al., 2016b). Rocks with high porosity and permeability allow water to penetrate through subsurface flows. Conversely, impermeable rocks obstruct infiltration and facilitate surface runoff (Benjmel et al., 2020). This study identified two lithological layers: Qe (Holocene), including unconsolidated sands, silts, and clays with variable water permeability, and T (Tertiary), consisting of sandstones and limestones that facilitate water movement, as seen in Fig. 10a. Tertiary received the maximum weight rank of "4", signifying its excellent groundwater potential, whereas Holocene was assigned a weighted value of "3", showing it also has substantial groundwater potential (Table 5).

3.9. Soil texture

Soil is the top layer of the Earth's surface that serves as a medium for water percolation. It is an essential component for identifying groundwater potential zones. The water retention capacity of an area depends on different soil types and permeability (Kumar et al., 2016c). The permeability of soil types depends on their texture. As a result, the soil types identified in the study region were adjusted from those listed in the FAO (2003)

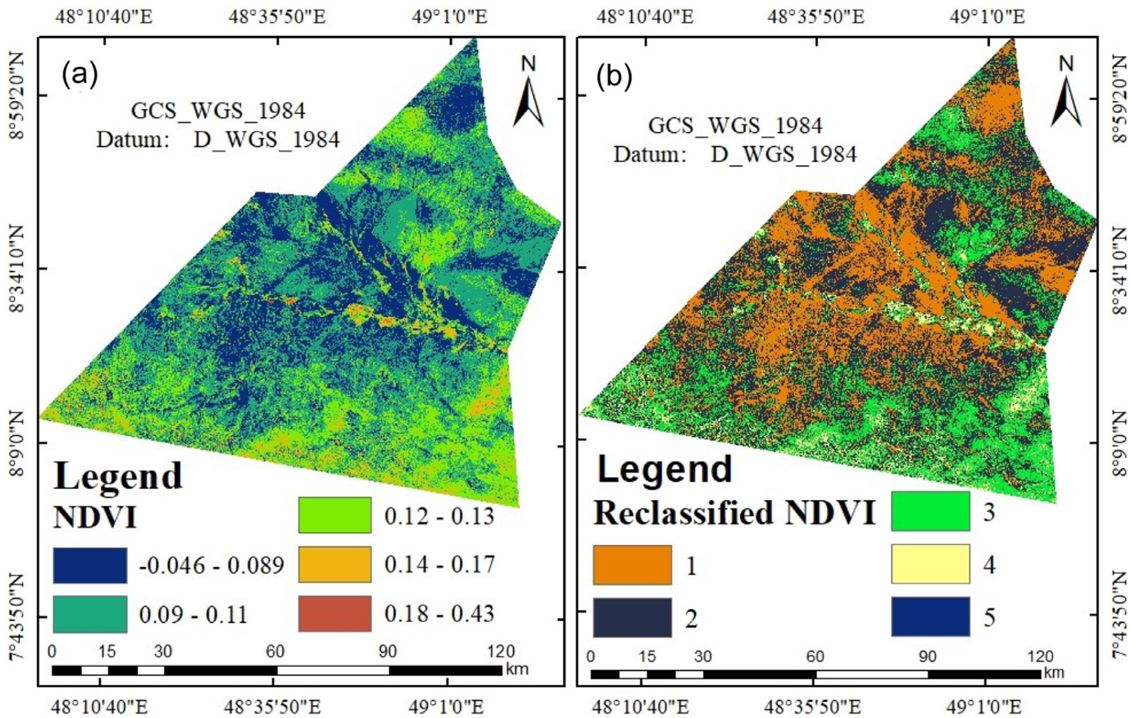

Fig. 9. Maps showing (a) NDVI and (b) reclassified NDVI.

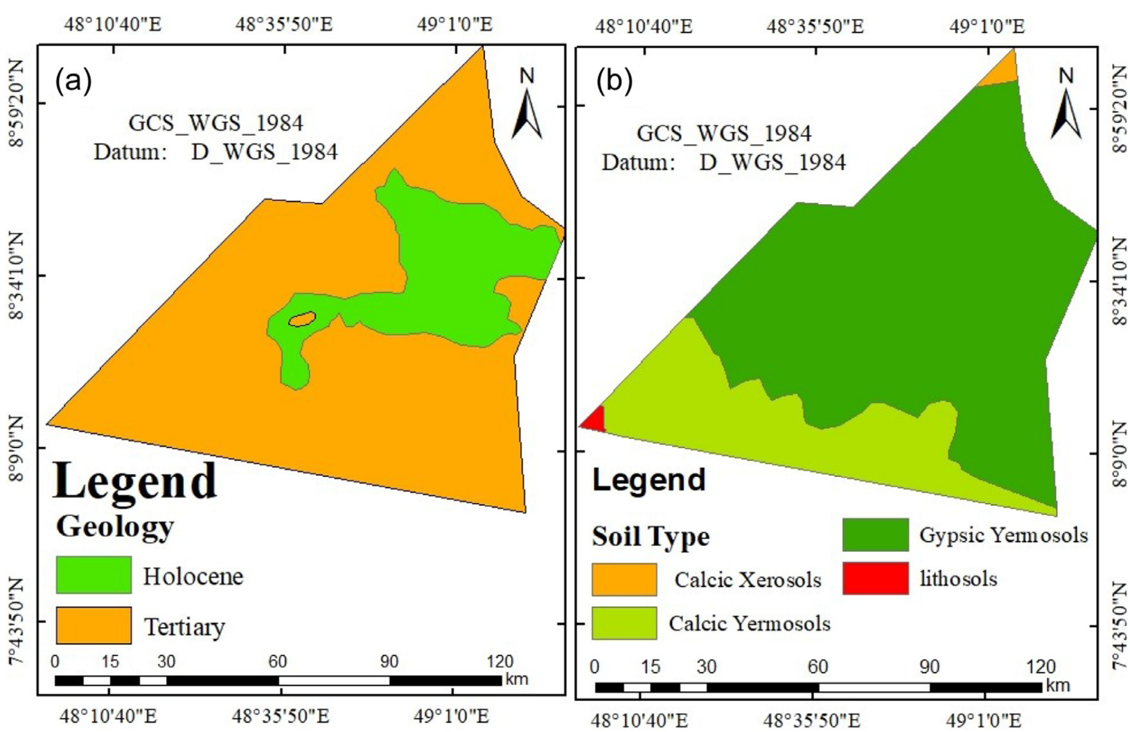

Fig. 10. Maps showing (a) geology and (b) soil types.

classification for this research to align with the USDA soil textural classification. Soil largely influences infiltration and percolation processes, which subsequently impact groundwater recharge and the groundwater potential of a specific area (Berhanu and Hatiye, 2020a). Alluvial soils increase recharge, thus enhancing the possibility for groundwater availability. Conversely, compacted soil conditions and fine-textured soils have less permeability, hence promoting surface runoff over subsurface flow (Rukundo and Doğan, 2019). This research identified the three soil types (Fig. 10b).

The Calcic Yermosols soil, characterized by the accumulation of calcium carbonate, $CaCO_3$, might affect the structure and movement of water within the soil. Calcic Yermosols have higher hydraulic conductivity than Gypsic Yermosols because of their granular structure and high porosity associated with the calcium carbonate content. This high hydraulic conductivity will promote water

Table 6
Pairwise comparison matrix of the selected thematic layers and their weights.

Matrix	Rainfall	Geology	Slope	Drainage density	Elevation	LULC	Lineament Density	Soil types	NDVI	Normalized weight	Normalized principal eigenvector	Checking of consistency ratios (CR)
Rainfall	1	3	3	5	5	5	7	5	7	0.286	28.65%	
Geology	1/3	1	1	2	3	6	5	5	5	0.156	15.66%	$\lambda_{max} = 9.748$
Slope	1/3	1	1	2	3	5	7	3	3	0.153	15.29%	CI = 0.0960
Drainage density	1/5	1/2	1/2	1	2	5	6	3	5	0.112	11.20%	RI = 1.45
Elevation	1/5	1/3	1/3	1/2	1	2	3	4	3	0.073	7.27%	CR = 0.0662
LULC	1/5	1/6	1/5	1/5	1/2	1	2	2	2	0.046	4.58%	CR < 0.1
Lineament density	1/7	1/5	1/7	1/6	1/3	1/2	1	3	5	0.040	3.97%	Consistency Ratio is acceptable
Soil types	1/5	1/5	1/3	1/3	1/4	1/2	1/3	1	7	0.036	3.58%	
NDVI	1/7	1/5	1/3	1/5	1/3	1/2	1/5	1/7	1	0.098	9.80%	
Total	2.75	6.6	6.8	11.4	15.4	25.5	31.8	26.2	38	1	100%	

Table 7
Normalized weight of the matrix.

Factor	Rainfall	Geology	Slope	Drainage density	Elevation	LULC	Lineament density	Soil types	NDVI	Eigen vector	Weights
Rainfall	0.37	0.45	0.44	0.44	0.32	0.19	0.22	0.19	0.18	0.286	28.65%
Geology	0.12	0.15	0.15	0.17	0.19	0.23	0.16	0.19	0.13	0.156	15.66%
Slope	0.12	0.15	0.14	0.17	0.19	0.19	0.22	0.11	0.08	0.153	15.29%
Drainage density	0.073	0.075	0.07	0.08	0.13	0.19	0.19	0.11	0.13	0.112	11.20%
Elevation	0.072	0.05	0.05	0.04	0.06	0.08	0.09	0.15	0.079	0.073	7.27%
LULC	0.072	0.025	0.03	0.02	0.03	0.04	0.06	0.07	0.052	0.046	4.58%
Lineament density	0.052	0.030	0.02	0.01	0.02	0.02	0.03	0.11	0.13	0.040	3.97%
Soil types	0.073	0.030	0.04	0.03	0.03	0.01	0.01	0.04	0.184	0.036	3.58%
NDVI	0.052	0.021	0.04	0.02	0.02	0.02	0.006	0.01	0.026	0.098	9.80%
Sum	1.00	1.00	1.00	1.00	1.00	1.00	1.00	1.00	1.00	1.00	100%

infiltration and result in a high potential for groundwater recharge. The hydraulic conductivity of Gypsic Yermosols tends to be moderate to low. The presence of gypsum can enhance soil structure and may lead to reducing its permeability when saturated, hence reducing infiltration rate, depending on the soil texture and compaction levels.

Lithosols, located on rocky substrates, usually have low water retention capacity, resulting in a decrease in the groundwater potential. Therefore, Calcic Xerosols obtained the highest rating of 5, Calcic Yermosols received a good score of 4, Gypsic Yermosols garnered a moderate rating of 3, and Lithosols received a low score of 2, impacting groundwater recharge, as depicted in Table 5.

3.10. Assignment of weightages to the thematic layers using AHP

The AHP analysis approach, using Satty's scale, was employed to categorize the identified thematic levels. Subsequently, we computed the pairwise comparison matrix based on the regime affecting groundwater (Table 6). The consistency index was then calculated, and the consistency ratio findings were analyzed. The thematic layers were subsequently assigned normalized weights based on their relevance (Table 6). AHP analysis was computed using the different equations explained in Section 2.4. Satty's technique assigns equal ratings to layers with similar influencing factors for groundwater targeting. A layer with more priority is assigned the highest rank. In this analysis, the rainfall layer has been assigned the highest weighting (28.65%), followed by Geology and Slope (Tables 6 and 7). Ranks were given to all selected layers, and pairwise comparison matrices were calculated Table 6. The lambda value is described as the consistency vector ($\lambda = 9.7480$). By using this vector value with the total number of criteria in Eq. (8), as referenced in Section 2.5, we determine the consistency index value. The consistency ratio (Cr) values were verified according to the random index values provided by Saaty's AHP template (Table 3). If Cr is <0.1, the allocated weights are valid and consistent. In this instance, CI = 0.0960 (derived from Eq. (12)) and RI = 1.45 (Saaty 1990; Saaty 2005; Table 3). Substituting these numbers into Eq. (11) in Section 2.5, a CR value is 0.06620, which is <0.1. The average values of normalized weights (Table 7) were finally allocated to the thematic layers in the weighted overlay analysis to delineate groundwater potential zones.

$$\boldsymbol{CI} = \frac{9.768 - 9}{9 - 1} = 0.0960 \tag{13}$$

3.11. Mapping of the groundwater potential zones

The AHP technique was utilized to determine suitable rankings and weights for nine thematic layers, which were then created within a GIS tool and designated for the overlay process. Groundwater potential index (GWPI) is a dimensionless measurement calculated based on the weights assigned to each layer and subclass within each thematic layer. GWPI was calculated using the weighted linear combination technique, as shown in Eqs. (11) and (14) (Tamesgen et al., 2023). Where m denotes the total number of thematic layers, n is the total number of classes in the j^{th} thematic layer, and X_i is the rate value of each class in the jth layer. The input datasets included nine classified raster-format themed maps. The assigned weight of each component has been set on a scale (Table 8). The overlay analysis method in the spatial analysis tool was conducted in ArcGIS 10.8 software using the following equation:

$$\begin{aligned} \mathrm{GWPI} = {} & 0.29\mathrm{Rf} + 0.16\mathrm{GLG} + 0.15\mathrm{Sl} + 0.11\mathrm{DD} + 0.73\mathrm{El} \\ & + 0.046\mathrm{LULC} + 0.04\mathrm{LD} + 0.036\mathrm{ST} + 0.098\mathrm{NDVI} \end{aligned} \tag{14}$$

where RF represents rainfall, GLG represents geology, Sl represents slope, DD represents drainage density, El represents elevation, LULC represents land use and land cover, LD represents lineament density, ST represents soil type, and NDVI represents the normalized difference vegetation index.

The results were categorized into five groups based on index value, ranging from Excellent potential zone to very poor poten-

Table 8
Summary of scores and weightage allocated to thematic layers influencing groundwater potential.

Thematic layer	Dominant feature	Suitability rank	Score	Weightage
	100–97	Very High	5	
Rainfall (mm)	96–93	High	4	29
	92–89	Moderate	3	
	88–83	Low	2	
	82–76	Very Low	1	
	Holocene	Moderate	3	15.7
Geology	Tertiary	High	4	
	48–18	Very Low	1	
Slope (Degree)	17–11	Low	2	15.3
	10–5.4	Moderate	3	
	5.3–2.4	High	4	
	2.3–0	Very High	5	
	1.4–1.2	Very Low	1	
Drainage density	1.1–0.83	Low	2	11.2
(km/km^2)	0.82–0.56	Moderate	3	
	0.55–0.29	High	4	
	0.28–0.0038	Very High	5	
	0.43–0.19	Very High	5	
NDVI	0.17–0.14	High	4	9.8
	0.13–0.12	Moderate	3	
	0.11–0.09	Low	2	
	0.089- (−0.046)	Very Low	1	
	840–700	Very low	1	
Elevation (m)	690–590	Low	2	7.3
	580–500	Moderate	3	
	490–410	High	4	
	400–280	Very High	5	
	Water	Very High	5	
LULC	Trees	Very High	5	4.6
	Crops	High	4	
	Rangeland	Moderate	3	
	Bare land	Low	2	
	Built area	Very Low	1	
	1.6–1.3	Very High	5	
Lineament density	1.2–0.94	High	4	4
(km/km^2)	0.93–0.63	Moderate	3	
	0.62–0.32	Low	2	
	0.31–0	Very Low	1	
	Calcic xerosols	Very High	5	
Soil type	Calcic yermosols	High	4	3.6
	Gypsic yermosols	Moderate	3	
	lithosols	Low	2	
Total				100%

Table 9
Groundwater potential zones and corresponding areal distribution.

No.	GWPZ	Area (km^2)	Percentage (%)
1	Excellent	685.16	7.87%
2	Very Good	2446.90	28.11%
3	Good	2383.5	27.48%
4	Poor	2069.9	23.77%
5	Very Poor	1116.8	12.83%
	Total	8702.3	100%

tial zone (Fig. 11 and Table 9). The groundwater potential map (Fig. 11) shows high potential groundwater locations, which are mainly within streams and rivers. This is mainly due to the presence of the high-yielding tertiary surface sediment aquifer on flat terrain. Some other areas of higher groundwater potential are situated in high- to very-high lineament density zones (0.94–1.2 km/km^2), low-slope zones (0°–2.3°), and poor drainage density zones (0.0038–0.28 km/km^2; Figs. 3,7, and 8). The Good groundwater potential zone is found in sloping terrain (2.4°–5.3°), flat or nearly flat plains, plains with significant hills, and regions characterized by gypsic yermolos soil type.

A small part of the good groundwater potential zone is also dispersed in the northwestern direction, characterized by a moderate lineament density (0.63–0.93 km/km^2). Areas of poor and very poor groundwater potential occur in the southern part of the study area. Possibly, this is because of the region's extensive mountainous geomorphology and comparatively low water-bearing lithological units. Conversely, the northwestern part of the study area contains an irregular distribution of this groundwater potential zone. The excellent and very good zones cover 685.16 km^2 and 2446.90 km^2, respectively, constituting 35.9% of the total study area. The good potential zone covers 2383.5 km^2, representing 27.5% of the overall research area, whereas the Poor and very Poor zones cover 3186.7 km^2, or 36.6%, of the total study area.

3.12. Validation of groundwater potential zones

The identified groundwater potential zones, using remote sensing, GIS, and AHP techniques, have been validated with existing groundwater data points. Validation is an important component of modeling; in its absence, results lack scientific significance (Godif and Manjunatha, 2023). A poor understanding of validation methodologies and variables can limit the effectiveness of remotely sensed data (Malczewski, 2006). The kappa coefficient was calculated to assess the degree of agreement between GPZs determined from nine hydrogeological parameters and inventory borehole data. The Kappa coefficient normally ranges from −1 to 1, with values approaching 1 signifying excellent agreement (Sahoo et al., 2024).

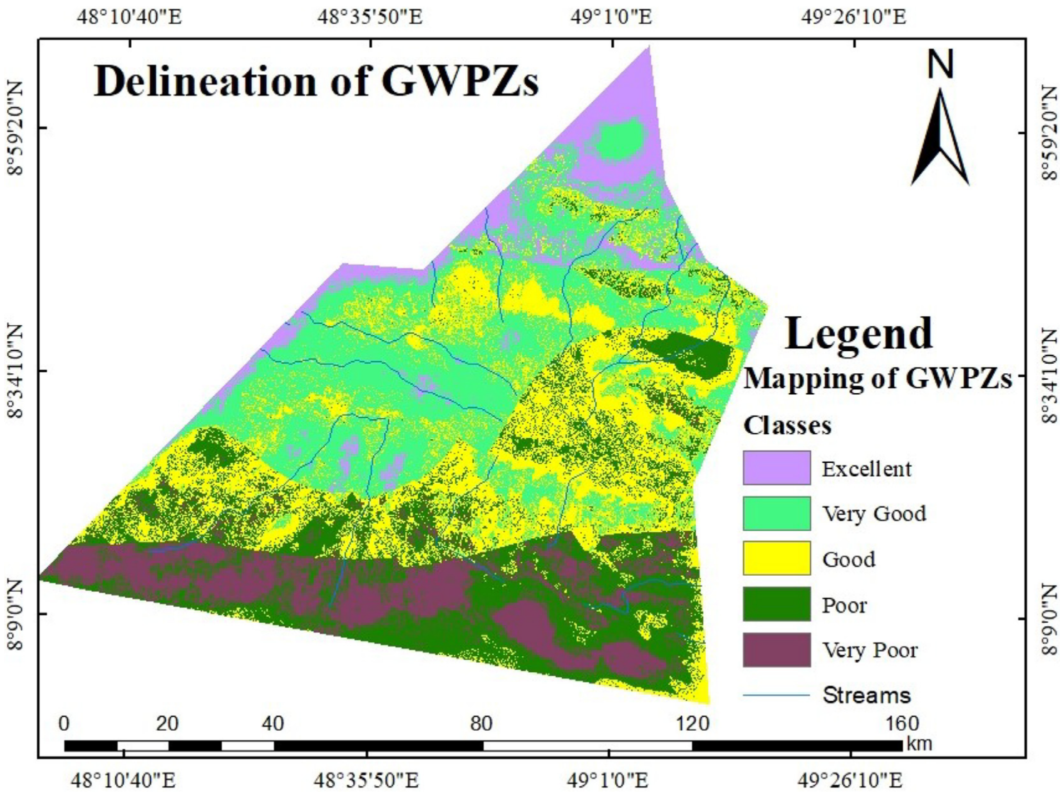

Fig. 11. Mapping of groundwater potential zones (GWPZs).

Table 10
Expressions of the Kappa coefficient agreement.

Range of the Kappa coefficient	Nature of agreement
$K < 0.00$	Poor agreement
$K \geq 0.20$	Slight agreement
$0.21 \leq k \geq 0.40$	Fair agreement
$0.41 \leq k \geq 0.60$	Moderate agreement
$0.61 \leq k \geq 0.80$	Good agreement
$0.80 \leq k \geq 1$	Very good agreement

Source: (Das et al., 2021).

This study utilized data from 50 inventory data points across the study area for validation, resulting in the generation of a confusion matrix and a kappa coefficient (Table 10). Nine of the total boreholes were founded in excellent groundwater protection zones (GWPZs), seventeen in very good GWPZs, eleven in Good GWPZs, nine in poor GWPZs, and four in very poor GWPZs (Table 11). Before conducting the validation procedure, the borehole yields were divided into five different groups. There is no conventional borehole yield classification system. Site observations, field expertise, researchers' experience, and hydrologists' recommendations are often considered (Saranya and Saravanan, 2020). Therefore, the borehole data of this study were classified based on information obtained from the Somalia Ministry of Water Resources and Energy (MOWRE), the Puntland Ministry of Water, Energy, and Mining (MOWEM), the Puntland Water Development Agency (PWDA), and the Puntland Information Management Center (IMC). The boreholes were classified as very Poor, Poor, Good, very Good, and Excellent based on yields of <2L/S, 3–6L/S, 7–10L/S, 11–20L/S, and >30L/S, respectively. Several techniques have been used in the overlay analysis. Initially, the validation points (boreholes) were organized in Excel format, along with their categorized yields and geographical coordinates. The Excel data was then imported into the ArcGIS platform and projected to WGS 1984 UTM Zone 39 N, a standard coordinate system compatible with the GIS-generated groundwater potential map. The predicted location points were then transformed into shapefile point data and overlaid on the produced groundwater potential map (Fig. 12). Raster values from the delineated groundwater potential map were extracted to the classified borehole yields using the "Extract Values to points" tool within the Spatial Analyst extension of ArcGIS to assess the degree of overlap. A frequency table was constructed using the "frequency" feature in ArcGIS's analysis tool extension to show the number of predictions that agreed with the validation points. Finally, an error matrix was generated from the data shown in the frequency table, using the "pivot table" feature in the data management tools of the ArcGIS extension. The Error Matrix includes a square array of numerical values organized in rows and columns, where the columns denote field data, and the rows indicate information derived from remotely sensed data. According to Congalton (1991), there are two acknowledged accuracy assessments: exclusion accuracy evaluation and inclusion accuracy assessment. The exclusion accuracy assessment reflects the likelihood that the validation ground data is accurately classified within the specified area. The inclusion accuracy assessment indicates the probability that the information derived from remotely sensed data accurately reflects the actual conditions on the ground (Story and Congalton, 1986). The objective of this study is to verify the probability that the identified groundwater potential corresponds to the actual borehole yield; thus, an accuracy assessment of inclusion was employed. Many researchers (Nigussie et al. 2019a; Berhanu and Hatiye, 2020a; Guduru and Jilo, 2022; Sahoo et al., 2024) used a similar approach to evaluate groundwater potential zones, with a focus on prospective locations for springs, hand-dug wells, and borehole yields. Table 11 shows the error matrix utilized for validation analysis. The matrix's rows signify the identified groundwater potential zones, the columns denote the categorized borehole yields, and the principal diagonal

Table 11
Kappa Statistics and Confusion Matrix result for GWPZ obtained with the AHP technique.

	Excellent	Very Good	Good	Poor	Very Poor	Row Total	User's accuracy
Excellent	6	1	0	0	0	7	**86%**
Very Good	3	13	0	0	0	16	**81%**
Good	0	3	8	0	1	12	**67%**
Poor	0	0	3	8	0	11	**73%**
Very Poor	0	0	0	1	5	6	**83%**
Colum Total	9	17	11	9	4	50	
Producer's accuracy	0.67%	0.82%	0.73%	0.89%	0.75%		
Overall accuracy	**0.80%**						
Kappa (K)	**0.74%**						

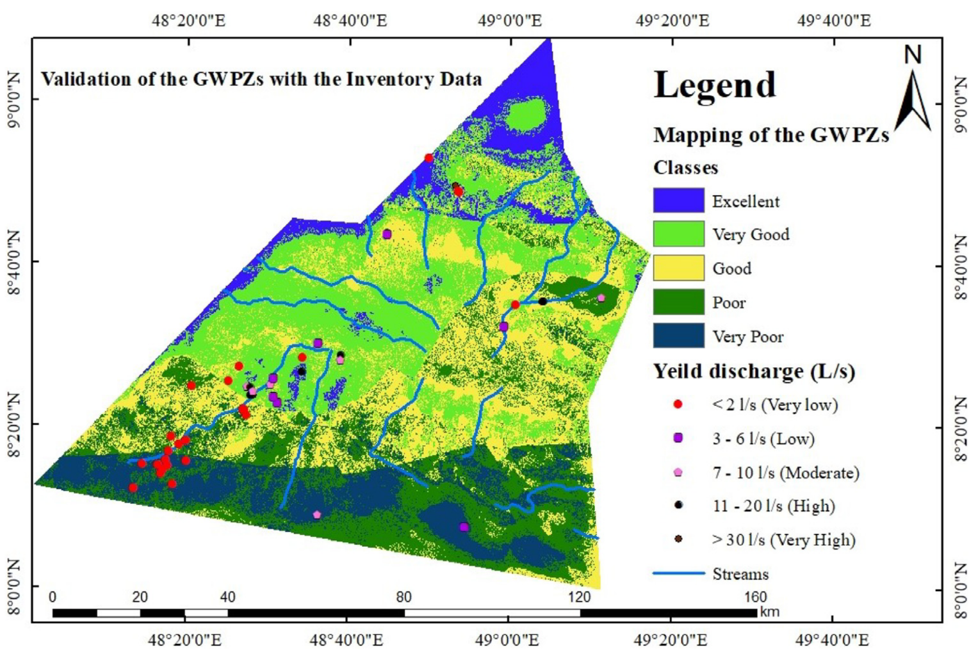

Fig. 12. Validation of GWPZ with Inventory data.

indicates the quantity of coinciding classified borehole values for each delineated groundwater potential zone. The percentage coincidence of individual borehole yield classes within each associated groundwater potential zone was calculated by dividing the number of coincident boreholes yields in each zone by the total number of rows and multiplying the result by 100. Therefore, 6 of 7 (85%) boreholes accurately coincided with the Excellent GWPZ, 13 of 16 (81%) boreholes coincided with the Very Good GWPZ, 8 of 12 (67%) boreholes accurately coincided with the Good GWPZ, 8 of 11 (73%) boreholes coincided with the Poor GWPZ, and 5 of 6 (83%) boreholes accurately coincided with the Very Poor GWPZ (Table 11). The overall accuracy (percentage of coincidence) was determined by dividing the sum of the principal diagonal elements of the error matrix (6 + 13 + 8 + 8 + 5 = 40) by the total number of boreholes 50 and multiplying by 100, as illustrated in Eq. (15):

$$\text{Overall accuracy \%} = \frac{\text{Sum of diagonal elements}}{\textit{Total number of samples}} \times 100 = \frac{40}{50} = 80\% \quad (15)$$

Therefore, the overall accuracy assessment of consistency between the identified groundwater potential zones utilizing the applied technique and actual ground data is 80%. Similarly, IBM SPSS 25 software was used to compute kappa statistics to validate GWPZ using borehole yield data, as illustrated in Eq. (16). The kappa statistic considers the probability of agreement via chance (Das et al., 2021). When two measures (actual yield and projected yield) coincide only at the level of chance, the kappa statistic is 0. When the two measurements coincide, the value of kappa is 1.0. The following formula has been used to compute the Kappa statistic value:

$$K = \frac{observed\ \ agreement - chance\ \ agreement}{1 - chance\ \ agreement} \quad (16)$$

Table 11 reveals that the Kappa statistic for the GWPZ map produced with the AHP method is 0.74%, while the overall accuracy is 0.80%. An agreement level above 0.7 is considered good for validation.

4. Limitation

In this study, we delineate the groundwater potential zones of the Garowe District semi-arid region of Puntland, Somalia. We carefully collected data from various sources and analyzed research results to identify areas of potential groundwater sources. We meticulously follow scientific research methodology to make sure our research results are more reliable. However, we faced some research limitations as listed below.

(1) This study faces a lack of complete groundwater inventory data; this constraint may reduce the analysis and limit the ability to draw a comprehensive conclusion.
(2) We also faced irregular distribution of data points across the study area, which may cause uncertainty during the validation process.

(3) This study faced financial resource and human limitations, which made it difficult to conduct an extensive field survey. We did not consider seasonal variations due to a lack of financial resources, logistics, and time, as well as a lack of a temporal data source and temporal irregularity.
(4) We used a limited number of existing data (50) to validate groundwater potential zones, which may not provide a comprehensive representation of the groundwater conditions across the entire study area.

5. Conclusions

This research used GIS, RS, and AHP approaches to evaluate groundwater potential zones (GWPZs) in Northeastern Somalia, focusing on the Garowe district. Thematic layers that substantially affect GWPZs, including land use/cover, lithology/geology, lineament density, slope, soil properties (texture and type), drainage density, rainfall, NDVI, and elevation, were generated utilizing available data from conventional sources and satellite imagery. Individual weights were given to the subclass categorizations based on literature, expert opinion, the researcher's experience, hydrogeologist, hydrologist, and geologist recommendations. The study revealed that over 35.98% (3132.06 km^2) of the research area had "very good" and "excellent" groundwater potential, while 27.48% (2383.5 km^2), 23.77% (2069.9 km^2), and 12.83% (1116.8 km^2) are categorized as "good," "poor," and "very poor," respectively, within the total area of the Garowe district (8702.3 km^2). Very Good to Excellent GWPZs were found in the middle, northern, and northeastern parts of the study area, which are locally referred to as "dhoodi," or groundwater-rich areas. On the other hand, the poor and very poor potential zones were in the southern and western parts of the study area, known as "hawd," water-scarce areas. Poor GWPZs might have been characterized by hills, steep slopes, escarpments, sloping ground, and solid rock ground. Based on the AHP weight analysis results, the combined weight of precipitation (28.65%), geology (15.66%), and slope (15.29%) exceeds 59.6%, making them the core factors controlling groundwater occurrence in the study area.

The study finally applied observed well discharge data to validate the results of the groundwater potential zone. The research demonstrates a robust overall assessment correlation coefficient of 80% and a Kappa statistic of 74%, indicating a high level of confidence. This research offers stakeholders, including the Garowe administration office, the region, and society, an efficient, time-saving, and rapid assessment of groundwater resources, providing evidence to enhance understanding of locations with varying groundwater levels for improved management of these vital resources. It may assist policymakers and planners in establishing policies for safeguarding, exploiting, and using accessible groundwater for multiple purposes. The groundwater potential zone map of the present study provides information to water stakeholders, local governments, and decision-makers to develop enhanced sustainable water use for urban and agricultural purposes in this region, thereby reducing costs, time, and human effort.

6. Recommendation

This study focuses on the determination of the groundwater potential zones in the Garowe district of Puntland, Somalia, a semi-arid region. We innovatively integrate remote sensing (RS), geographic information systems (GIS), and the analytical hierarchy process (AHP) to delineate groundwater potential zones (GWPZ). We used nine thematic parameters influencing the groundwater potential areas; therefore, we recommend future studies to increase the number of criteria to enhance the accuracy of the prediction. We also suggested expanding the study area to include other semi-arid regions. In this study, we used GIS-based AHP techniques, so we recommended that future scholars consider a combination of machine learning algorithms (MLA), frequency ratio (FR), certainty factor (CF), and index models (IM), and AHP models to make a groundwater potential zone map for a more comprehensive understanding of the spatial distribution of the potential groundwater zone in the studied area under different models. We found that the rainfall, geology, and slope are the main influence parameters; therefore, we recommended a future study to explore the differences in groundwater recharge efficiency of different geological units under different rainfall intensities and slope conditions. Additionally, we recommended that future researchers consider hydrogeological field surveys as well as numerical simulation methods (e.g., MODFLOW) to predict groundwater dynamic changes. Since the study area is located semi-arid region, we suggested that future researchers explore long-term climate data observation to analyze the spatiotemporal trend of groundwater potential in the study area under climate change scenarios. Furthermore, we recommended consideration of the quality of the groundwater along with the suitability of the potential areas. Finally, we suggest adopting alternative sources of water, such as rainwater harvesting in poor groundwater potential areas, to reduce excessive reliance on groundwater.

Data availability

The data source of this study will be made available on request via a.moha1010@gmail.com.

Declaration of competing interest

The authors declare that they have no known competing financial interests or personal relationships that could have appeared to influence the work reported in this paper.

CRediT authorship contribution statement

Ahmed Mohamed Ismail: Writing – review & editing, Writing – original draft, Visualization, Validation, Supervision, Software, Resources, Project administration, Methodology, Investigation, Funding acquisition, Formal analysis, Data curation, Conceptualization. **Farah Jama Farah:** Writing – review & editing, Validation, Supervision, Methodology, Formal analysis, Data curation, Conceptualization. **Mohamed Abdi Jama:** Writing – review & editing, Visualization, Validation, Supervision, Methodology, Conceptualization. **Rodgers Makwinja:** Writing – review & editing, Visualization, Validation, Supervision, Investigation, Data curation, Conceptualization. **Yoshihiko Inagaki:** Writing – review & editing, Visualization, Validation, Supervision, Methodology, Data curation, Conceptualization.

Acknowledgements

The author expresses gratitude for the support received from various organizations, including the Somalia Ministry of Water Resources and Energy (MOWRE), Nugal Water Company (NUWACO), the Puntland Ministry of Water, Energy, and Mining (MOWEM), the Puntland Water Development Agency (PWDA), the Puntland Information Management Center (IMC), and the Garowe District Municipality Administration Office. We finally thank all constructive comments and suggestions provided by the two anonymous reviewers and the editor, which have helped improve the quality of the manuscript.

References

Athick, Abdul, Mohammed, A.S., Shankar, K., 2019a. Data on land use and land cover changes in Adama Wereda, Ethiopia, on ETM+, TM and OLI- TIRS landsat sensor using PCC and CDM techniques. Data Brief 24. doi:10.1016/j.dib.2019.103880.

Athick, Abdul, Mohammed, A.S., Shankar, K., Naqvi, Hasan Raja, 2019b. Data on time series analysis of land surface temperature variation in response to vegetation indices in twelve wereda of Ethiopia using mono window, split window algorithm and spectral radiance model. Data Brief 27. doi:10.1016/j.dib.2019.104773.
Abdullahi, Ahmed, Jothimani, Muralitharan, Getahun, Ephrem, Gunalan, Jagadeshan, Abebe, Abel, 2023a. Assessment of potential groundwater zones in the drought-prone Harawa catchment, Somali Region, eastern Ethiopia using geospatial and AHP techniques. Egyptian Journal of Remote Sensing and Space Science 26 (3), 628–641. doi:10.1016/j.ejrs.2023.07.005.
Abdullahi, Ahmed, Jothimani, Muralitharan, Getahun, Ephrem, Gunalan, Jagadeshan, Abebe, Abel, 2023b. Assessment of potential groundwater zones in the drought-prone Harawa catchment, Somali Region, eastern Ethiopia using geospatial and AHP techniques. Egyptian Journal of Remote Sensing and Space Science 26 (3), 628–641. doi:10.1016/j.ejrs.2023.07.005.
Adiat, K.A.N., Nawawi, M.N.M., Abdullah, K., 2012. Assessing the accuracy of GIS-based elementary multi criteria decision analysis as a spatial prediction tool - A case of predicting potential zones of sustainable groundwater resources. J Hydrol 440–441, 75–89. doi:10.1016/j.jhydrol.2012.03.028.
Aju, C.D., Achu, A.L., Raicy, M.C., Reghunath, Rajesh, 2021a. Identification of suitable sites and structures for artificial groundwater recharge for sustainable water resources management in Vamanapuram River Basin, South India. HydroResearch 4, 24–37. doi:10.1016/j.hydres.2021.04.001.
Aju, C.D., Achu, A.L., Raicy, M.C., Reghunath, Rajesh, 2021b. Identification of suitable sites and structures for artificial groundwater recharge for sustainable water resources management in Vamanapuram River Basin, South India. HydroResearch 4, 24–37. doi:10.1016/j.hydres.2021.04.001.
Ally, Ally Mgelwa, Yan, Jianguo, Bennett, George, Lyimo, Neema Nicodemus, Mayunga, Selassie David, 2024a. Assessment of groundwater potential zones using remote sensing and GIS-based fuzzy analytical hierarchy process (F-AHP) in Mpwapwa District, Dodoma, Tanzania. Geosystems and Geoenvironment 3 (1). doi:10.1016/j.geogeo.2023.100232.
Ally, Ally Mgelwa, Yan, Jianguo, Bennett, George, Lyimo, Neema Nicodemus, Mayunga, Selassie David, 2024b. Assessment of groundwater potential zones using remote sensing and GIS-based fuzzy analytical hierarchy process (F-AHP) in Mpwapwa District, Dodoma, Tanzania. Geosystems and Geoenvironment 3 (1). doi:10.1016/j.geogeo.2023.100232.
Alshehri, Fahad, El-Hamid, Hazem T.Abd, Mohamed, Ahmed, 2024. Mapping coastal groundwater potential zones using remote sensing based AHP model in Al Qunfudhah Region along Red Sea, Saudi Arabia. Heliyon 10 (7). doi:10.1016/j.heliyon.2024.e28186.
Alshehri, Fahad, Abdelrahman, Kamal, 2023. Groundwater potentiality of Wadi Fatimah, western Saudi Arabia: geophysical and remote sensing integrated approach. Water (Switzerland) 15 (10). doi:10.3390/w15101828.
Andualem, Tesfa Gebrie, Demeke, Girum Getachew, 2019a. Groundwater potential assessment using GIS and remote sensing: a case study of Guna Tana landscape, Upper Blue Nile Basin, Ethiopia. Journal of Hydrology: Regional Studies 24. doi:10.1016/j.ejrh.2019.100610.
Andualem, Tesfa Gebrie, Demeke, Girum Getachew, 2019b. Groundwater potential assessment using GIS and remote sensing: a case study of Guna Tana landscape, Upper Blue Nile Basin, Ethiopia. Journal of Hydrology: Regional Studies 24. doi:10.1016/j.ejrh.2019.100610.
Araya, Dahyann, Podgorski, Joel, Berg, Michael, 2023a. Groundwater salinity in the Horn of Africa: spatial prediction modeling and estimated people at risk. Environ Int 176. doi:10.1016/j.envint.2023.107925.
Araya, Dahyann, Podgorski, Joel, Berg, Michael, 2023b. Groundwater salinity in the Horn of Africa: spatial prediction modeling and estimated people at risk. Environ Int 176. doi:10.1016/j.envint.2023.107925.
Balasubramani, Karuppusamy., 2018. Physical resources assessment in a semi-arid watershed: an integrated methodology for sustainable land use planning. ISPRS Journal of Photogrammetry and Remote Sensing 142, 358–379. doi:10.1016/j.isprsjprs.2018.03.008.
Ban, Yifang, Gong, Peng, Giri, Chandra, 2015. Global land cover mapping using earth observation satellite data: recent progresses and challenges. ISPRS Journal of Photogrammetry and Remote Sensing 103, 1–6.
Benjmel, Khalid, Amraoui, Fouad, Boutaleb, Said, Ouchchen, Mohammed, Tahiri, Amine, Touab, Amine, 2020. Mapping of groundwater potential zones in crystalline terrain using remote sensing, GIS techniques, and multicriteria data analysis (Case of the Ighrem Region, Western Anti-Atlas, Morocco). Water (Switzerland) 12 (2). doi:10.3390/w12020471.
Berhanu, Kibrit Gedam, Hatiye, Samuel Dagalo, 2020a. Identification of groundwater potential zones using proxy data: case study of Megech Watershed, Ethiopia. Journal of Hydrology: Regional Studies 28. doi:10.1016/j.ejrh.2020.100676.
Berhanu, Kibrit Gedam, Hatiye, Samuel Dagalo, 2020b. Identification of groundwater potential zones using proxy data: case study of Megech Watershed, Ethiopia. Journal of Hydrology: Regional Studies 28. doi:10.1016/j.ejrh.2020.100676.
Chowdary, V.M., Chakraborthy, D., Jeyaram, A., Krishna Murthy, Y.V.N., Sharma, J.R., Dadhwal, V.K., 2013. Multi-criteria decision making approach for watershed prioritization using analytic hierarchy process technique and GIS. Water Resources Management 27 (10), 3555–3571. doi:10.1007/s11269-013-0364-6.
Congalton, Russell G., 1991. A review of assessing the accuracy of classifications of remotely sensed data. Remote Sens Environ 37 (1), 35–46. doi:10.1016/0034-4257(91)90048-B.
Das, Niladri, Mondal, Prolay, Sutradhar, Subhasish, Ghosh, Ranajit, 2021. Assessment of variation of land use/land cover and its impact on land surface temperature of asansol subdivision. The Egyptian Journal of Remote Sensing and Space Science 24 (1), 131–149. doi:10.1016/J.EJRS.2020.05.001.
Das, Sumit., 2019a. Comparison among influencing factor, frequency ratio, and analytical hierarchy process techniques for groundwater potential zonation in Vaitarna Basin, Maharashtra, India. Groundwater for Sustainable Development 8, 617–629. doi:10.1016/j.gsd.2019.03.003.
Das, Sumit., 2019b. Comparison among influencing factor, frequency ratio, and analytical hierarchy process techniques for groundwater potential zonation in Vaitarna Basin, Maharashtra, India. Groundwater for Sustainable Development 8, 617–629. doi:10.1016/j.gsd.2019.03.003.
Debela, Debisa, Wodessa, Fikadu Woldemariyam, Karuppannan, Shankar, Diriba, Dechasa, 2025a. Geospatial technology-based identification of groundwater potential zone in the Upper Dawa River Basin, southern Ethiopia. Scientific African 28, e02747. doi:10.1016/j.sciaf.2025.e02747.
Debela, Debisa, Wodessa, Fikadu Woldemariyam, Karuppannan, Shankar, Diriba, Dechasa, 2025b. Geospatial technology-based identification of groundwater potential zone in the Upper Dawa River Basin, southern Ethiopia. Scientific African 28, e02747. doi:10.1016/j.sciaf.2025.e02747.
Deepika, B., Avinash, Kumar, Jayappa, K.S., 2013. Integration of hydrological factors and demarcation of groundwater prospect zones: insights from remote sensing and GIS techniques. Environ Earth Sci 70 (3), 1319–1338. doi:10.1007/s12665-013-2218-1.
Diriba, Dechasa, Karuppannan, Shankar, Takele, Tariku, Husein, Musa, 2024. Delineation of groundwater potential zonation using geoinformatics and AHP techniques with remote sensing data. Heliyon 10 (3). doi:10.1016/j.heliyon.2024.e25532.
Godif, Gebremedhin, Manjunatha, B.R., 2023. Delineation of groundwater potential zones using remotely sensed data and GIS-based analytical hierarchy process: insights from the Geba River Basin in Tigray, Northern Ethiopia. Journal of Hydrology: Regional Studies 46. doi:10.1016/j.ejrh.2023.101355.
Golla, Veeraswamy, Etikala, Balaji, Veeranjaneyulu, Ala, Subbarao, M., Surekha, A., Narasimhlu, K., 2018. Data sets on delineation of groundwater potential zones identified by geospatial tool in Gudur Area, Nellore District, Andhra Pradesh, India. Data Brief 20, 1984–1991. doi:10.1016/j.dib.2018.09.054.
Gómez, Cristina, White, Joanne C., Wulder, Michael A., 2016. Optical remotely sensed time series data for land cover classification: a review. ISPRS Journal of Photogrammetry and Remote Sensing 116, 55–72.
Guddeti, Sravya Sai, Kurakalva, Rama Mohan, Karuppannan, Shankar, 2024. Identification of vulnerable areas using geospatial technologies in the Lower Manair River Basin of Telangana, Southern India. Geomatics, Natural Hazards and Risk 15 (1). doi:10.1080/19475705.2023.2296379.
Guduru, Jerjera Ulu, Jilo, Nura Boru, 2022. Groundwater potential zone assessment using integrated analytical hierarchy process-geospatial driven in a GIS environment in Gobele Watershed, Wabe Shebele River Basin, Ethiopia. Journal of Hydrology: Regional Studies 44. doi:10.1016/j.ejrh.2022.101218.
Hassan, Ahmed Mohamed, and Kerstin Danert. 2021. *A Sectoral Analysis Water+ in Somalia An Accompanying Report (of a Suite of Six Reports) with Economics of Water: Digging for Data-Towards Understanding Water as a Limiting or Enabling Factor for Socioeconomic Growth in Somalia*.
He, Binbin, Xing, Minfeng, Bai, Xiaojing, 2014. A synergistic methodology for soil moisture estimation in an Alpine prairie using radar and optical satellite data. Remote Sens (Basel) 6 (11), 10966–10985. doi:10.3390/rs61110966.
Ibrahim-Bathis, K., Ahmed, S.A., 2016a. Geospatial technology for delineating groundwater potential zones in Doddahalla Watershed of Chitradurga District, India. Egyptian Journal of Remote Sensing and Space Science 19 (2), 223–234. doi:10.1016/j.ejrs.2016.06.002.
Ibrahim-Bathis, K., Ahmed, S.A., 2016b. Geospatial technology for delineating groundwater potential zones in Doddahalla Watershed of Chitradurga District, India. Egyptian Journal of Remote Sensing and Space Science 19 (2), 223–234. doi:10.1016/j.ejrs.2016.06.002.
Rather, Javeed Ahmad, Andrabi, Zameer A.B.Raouf, 2012. Fuzzy logic based GIS modeling for identification of ground water potential zones in the Jhagrabaria Watershed of Allahabad District, Uttar Pradesh, India. Int. Journal of Advances in Remote Sensing and GIS. 1 (2), 218–233.
Jenifer, M.Annie, Jha, Madan K., 2017. Comparison of analytic hierarchy process, catastrophe and entropy techniques for evaluating groundwater prospect of hard-rock aquifer systems. J Hydrol 548, 605–624. doi:10.1016/j.jhydrol.2017.03.023.
Khushi, Mudassar, Raza, Danish, Kamran, Muhammad, Nazeer, Majid, Ahmad, Adeel, Ullah Khan, Sami, Younas, Imtiyaz, 2023. Delineation of groundwater potential zones with analytic hierarchy process based geospatial modelling approach in metropolitan expanse. Desalination Water Treat 315, 399–412. doi:10.5004/dwt.2023.30155.
Kumar, Pankaj, Herath, Srikantha, Avtar, Ram, Takeuchi, Kazuhiko, 2016a. Mapping of groundwater potential zones in Killinochi Area, Sri Lanka, using GIS and remote sensing techniques. Sustain Water Resour Manag 2 (4), 419–430. doi:10.1007/s40899-016-0072-5.
Kumar, Pankaj, Herath, Srikantha, Avtar, Ram, Takeuchi, Kazuhiko, 2016b. Mapping of groundwater potential zones in Killinochi Area, Sri Lanka, using GIS and remote sensing techniques. Sustain Water Resour Manag 2 (4), 419–430. doi:10.1007/s40899-016-0072-5.
Kumar, Pankaj, Herath, Srikantha, Avtar, Ram, Takeuchi, Kazuhiko, 2016c. Mapping of groundwater potential zones in Killinochi Area, Sri Lanka, using GIS and remote sensing techniques. Sustain Water Resour Manag 2 (4), 419–430. doi:10.1007/s40899-016-0072-5.
Lavanya, M., Muthukumar, M., 2024. AHP and Geospatial technologies for identifying groundwater exploration target regions in Dindigul, Southern India. Geosystems and Geoenvironment, 100315 doi:10.1016/j.geogeo.2024.100315.

Li, Suxiao, Yang, Hong, Lacayo, Martin, Liu, Junguo, Lei, Guangchun, 2018. Impacts of land-use and land-cover changes on water yield: a case study in Jing-Jin-Ji, China. Sustainability (Switzerland) 10 (4). doi:10.3390/su10040960.

Jacek, Malczewsk, 1999. GIS and Multicriteria Decision Analysis, by Jacek Malczewski, 1999. Geogr Anal 34 (1), 91–92. doi:10.1111/j.1538-4632.2002.tb01077.x.

Malczewski, Jacek., 2006. GIS-based Multicriteria Decision Analysis: a survey of the literature. International Journal of Geographical Information Science 20 (7), 703–726. doi:10.1080/13658810600661508.

Mansaray, Lamin R., Huang, Weijiao, Zhang, Dongdong, Huang, Jingfeng, Li, Jun, 2017. Mapping rice fields in urban Shanghai, Southeast China, using sentinel-1A and landsat 8 datasets. Remote Sens (Basel) 9 (3). doi:10.3390/rs9030257.

Mishra, Deeksha, Singh, B.N., 2019. Identification of groundwater prospect in Bara Region of Allahabad district based on hydro-geomorphological analysis using satellite imagery. Journal of the Indian Society of Remote Sensing 47 (7), 1257–1273. doi:10.1007/s12524-019-00984-w.

Mohammed, Awol, Takele, Tariku, Mechal, Abraham, Jothimani, Muralitharan, 2025. Geospatial and satellite gravity-based assessment of groundwater potential in the Borkena Watershed, Northern Ethiopia. Journal of Hydrology: Regional Studies 62, 102828. doi:10.1016/j.ejrh.2025.102828.

Murmu, Preetilata, Kumar, Mukesh, Lal, Deepak, Sonker, Irjesh, Singh, Sudhir Kumar, 2019. Delineation of groundwater potential zones using geospatial techniques and analytical hierarchy process in Dumka District, Jharkhand, India. Groundwater for Sustainable Development 9, 100239. doi:10.1016/J.GSD.2019.100239.

Ndhlovu, George Z., Woyessa, Yali E., 2021. Integrated assessment of groundwater potential using geospatial techniques in Southern Africa: a case study in the Zambezi River Basin. Water (Switzerland) 13 (19). doi:10.3390/w13192610.

Nigussie, Wondifraw, Tesfaw Hailu, Binyam, Azagegn, Tilahun, 2019a. Mapping of groundwater potential zones using sentinel satellites (−1 SAR and -2A MSI) images and analytical hierarchy process in Ketar Watershed, Main Ethiopian Rift. Journal of African Earth Sciences 160. doi:10.1016/j.jafrearsci.2019.103632.

Nigussie, Wondifraw, Tesfaw Hailu, Binyam, Azagegn, Tilahun, 2019b. Mapping of groundwater potential zones using sentinel satellites (−1 SAR and -2A MSI) images and analytical hierarchy process in Ketar Watershed, Main Ethiopian Rift. Journal of African Earth Sciences 160. doi:10.1016/j.jafrearsci.2019.103632.

Owolabi, Solomon Temidayo, Madi, Kakaba, Kalumba, Ahmed Mulakazi, Orimoloye, Israel Ropo, 2020. A groundwater potential zone mapping approach for semi-arid environments using remote sensing (RS), geographic information system (GIS), and analytical hierarchical process (AHP) techniques: a case study of Buffalo Catchment, Eastern Cape, South Africa. Arabian Journal of Geoscience doi:10.1007/s12517-020-06166-0/Published.

Pande, Chaitanya B., Moharir, Kanak N., Panneerselvam, Balamurugan, Singh, Sudhir Kumar, Elbeltagi, Ahmed, Pham, Quoc Bao, Varade, Abhay M., Rajesh, J., 2021. Delineation of groundwater potential zones for sustainable development and planning using analytical hierarchy process (AHP), and MIF techniques. Appl Water Sci 11 (12). doi:10.1007/s13201-021-01522-1.

Rahim, Osama Abdul, Yin, Hailong, Ullah, Sajid, Durrani, Ayesha Noor, 2025. Delineation of groundwater potential zones and recharge using multi-source big data and systematic analysis approach. Sustainable Futures 10. doi:10.1016/j.sftr.2025.100872.

Rasool, Umair, Chen, Jianping, Muhammad, Shafi, Siddique, Jamil, Venkatramanan, Senapathi, Sabarathinam, Chidambaram, Siddique, Muhammad Amir, Rasool, Muhammad Awais, 2020. Geoinformatics and geophysical survey-based estimation of best groundwater potential sites through surface and subsurface indicators. Arabian Journal of Geosciences 13 (15). doi:10.1007/s12517-020-05496-3.

Riley, Dylan, Mieno, Taro, Schoengold, Karina, Brozović, Nicholas, 2019. The impact of land cover on groundwater recharge in the High Plains: an application to the Conservation Reserve program. Science of the Total Environment 696. doi:10.1016/j.scitotenv.2019.133871.

Rukundo, Emmanuel, Doğan, Ahmet, 2019. Dominant influencing factors of groundwater recharge spatial patterns in Ergene River catchment, Turkey. Water (Switzerland) 11 (4). doi:10.3390/w11040653.

Saaty, Thomas L., 1990. How to make a decision: the analytic hierarchy process. Eur J Oper Res 48 (1), 9–26. doi:10.1016/0377-2217(90)90057-I.

Saaty, Thomas L., 2005. Analytic hierarchy process. Encyclopedia of Biostatistics. Wiley.

Sahoo, Abinash, Subhadarshini, Rupsa, Baliarsingh, Falguni, 2024. Mapping of groundwater potential zones of Khordha District using GIS and AHP approaches. Cleaner Water 1, 100015. doi:10.1016/j.clwat.2024.100015.

Sar, Nityananda, Khan, Ansar, Chatterjee, Soumendu, Das, Arosikha, 2015. Hydrologic delineation of ground water potential zones using geospatial technique for Keleghai River Basin, India. Modeling Earth Systems and Environment 1 (3). doi:10.1007/s40808-015-0024-3.

Saranya, Thiyagarajan, Saravanan, Subbarayan, 2020. Groundwater potential zone mapping using analytical hierarchy process (AHP) and GIS for Kancheepuram District, Tamilnadu, India. Modeling Earth Systems and Environment 6 (2), 1105–1122. doi:10.1007/s40808-020-00744-7.

Senanayake, I.P., Dissanayake, D.M.D.O.K., Mayadunna, B.B., Weerasekera, W.L., 2016. An approach to delineate groundwater recharge potential sites in Ambalantota, Sri Lanka using GIS techniques. Geoscience Frontiers 7 (1), 115–124. doi:10.1016/j.gsf.2015.03.002.

Snapir, B., Hobbs, S., Waine, T.W., 2014. Roughness measurements over an agricultural soil surface with structure from motion. ISPRS Journal of Photogrammetry and Remote Sensing 96, 210–223. doi:10.1016/j.isprsjprs.2014.07.010.

Sreedevi, P.D., Sarah, S., Alam, Fakhre, Ahmed, Shakeel, Chandra, S., Pavelic, Paul, 2015. Investigating geophysical and hydrogeological variabilities and their impact on water resources in the context of Meso-watersheds. In: Integrated Assessment of Scale Impacts of Watershed Intervention: Assessing Hydrogeological and Bio-Physical Influences On Livelihoods. Elsevier Ltd, pp. 57–83.

Story, Michael, Congalton, Russell G., 1986. Accuracy Assessment: A User's Perspective.

Subramani, Deepa, Kamaraj, Pradeep, 2024. Groundwater exploration for sustainable development and management in a Hard Rock basin. Applied and Environmental Soil Science 2024. doi:10.1155/2024/7769047.

Subramani, Deepa, Kamaraj, Pradeep, Saravana Kumar, Umayadoss, Sabarathinam, Chidambaram, 2024. Mapping of groundwater recharge zones in hard rock aquifer through analytic hierarchy process in geospatial platform. Water (Switzerland) 16 (11). doi:10.3390/w16111484.

Sutradhar, Subhasish, Mondal, Prolay, Das, Niladri, 2021a. Delineation of groundwater potential zones using MIF and AHP models: a micro-level study on Suri Sadar Sub-Division, Birbhum District, West Bengal, India. Groundwater for Sustainable Development 12. doi:10.1016/j.gsd.2021.100547.

Sutradhar, Subhasish, Mondal, Prolay, Das, Niladri, 2021b. Delineation of groundwater potential zones using MIF and AHP models: a micro-level study on Suri Sadar Sub-Division, Birbhum District, West Bengal, India. Groundwater for Sustainable Development 12. doi:10.1016/j.gsd.2021.100547.

Tamesgen, Yohanis, Atlabachew, Abunu, Jothimani, Muralitharan, 2023. Groundwater potential assessment in the Blue Nile River catchment, Ethiopia, using geospatial and multi-criteria decision-making techniques. Heliyon 9 (6). doi:10.1016/j.heliyon.2023.e17616.

Tesfa, Chalachew, Sewnet, Demeke, 2025. Groundwater potential zonation mapping using GIS-based MCDM approach in East Gojjam Zone, Central Ethiopia. Journal of Hydrology: Regional Studies 60, 102494. doi:10.1016/j.ejrh.2025.102494.

Thomas, Renie, Duraisamy, Vijayasekaran, 2018. Hydrogeological delineation of groundwater vulnerability to droughts in semi-arid areas of western Ahmednagar District. Egyptian Journal of Remote Sensing and Space Science 21 (2), 121–137. doi:10.1016/j.ejrs.2016.11.008.

Upadhyay, Ritambhara K., Tripathi, Gaurav, Đurin, Bojan, Šamanović, Sanja, Cetl, Vlado, Kishore, Naval, Sharma, Mukta, Singh, Suraj Kumar, Kanga, Shruti, Wasim, Md, Rai, Praveen Kumar, Bhardwaj, Vinay, 2023. Groundwater potential zone mapping in the Ghaggar River Basin, North-West India, using integrated remote sensing and GIS techniques. Water (Switzerland) 15 (5). doi:10.3390/w15050961.

Verma, Narender, Patel, Ramesh Kumar, 2021. Delineation of groundwater potential zones in Lower Rihand River Basin, India using geospatial techniques and AHP. Egyptian Journal of Remote Sensing and Space Science 24 (3), 559–570. doi:10.1016/j.ejrs.2021.03.005.

Yeh, Hsin Fu, Cheng, Youg Sin, Lin, Hung I., Lee, Cheng Haw, 2016a. Mapping groundwater recharge potential zone using a GIS approach in Hualian River, Taiwan. Sustainable Environment Research 26 (1), 33–43. doi:10.1016/j.serj.2015.09.005.

Yeh, Hsin Fu, Cheng, Youg Sin, Lin, Hung I., Lee, Cheng Haw, 2016b. Mapping groundwater recharge potential zone using a GIS approach in Hualian River, Taiwan. Sustainable Environment Research 26 (1), 33–43. doi:10.1016/j.serj.2015.09.005.

Zewdie, Mulusew Minuyelet, Tesfa, Chalachew, 2023. GIS-based MCDM modeling for suitable dam site identification at Yeda Watershed, Ethiopia. Arabian Journal of Geosciences 16 (6). doi:10.1007/s12517-023-11409-x.